Diachronous Variscan tectonothermal activity in the NW Iberian Massif: Evidence from $^{40}Ar/^{39}Ar$ dating of regional fabrics

R.D. Dallmeyer [a], J.R. Martínez Catalán [b,*], R. Arenas [c], J.I. Gil Ibarguchi [d], G. Gutiérrez Alonso [b], P. Farias [e], F. Bastida [e], J. Aller [e]

[a] *Department of Geology, University of Georgia, Athens, GA 30602, USA*
[b] *Departamento de Geología, Universidad de Salamanca, 37008 Salamanca, Spain*
[c] *Departamento de Petrología y Geoquímica, Universidad Complutense, 28040 Madrid, Spain*
[d] *Departamento de Mineralogía–Petrología, Universidad del País Vasco, 48080 Bilbao, Spain*
[e] *Departamento de Geología, Universidad de Oviedo, 33005 Oviedo, Spain*

Abstract

Multigrain concentrates of hornblende and muscovite together with whole-rock slate/phyllite samples have been dated (27 analyses) using $^{40}Ar/^{39}Ar$ incremental-release methods along a systematic traverse across the various lithotectonic structural elements which comprise northwestern sectors of the Variscan Iberian Massif. Hornblende concentrates from amphibolites in the allochthonous Ordenes Complex yield plateau isotope-correlation ages of 425 Ma and 377 Ma. Muscovite concentrates and whole-rock slate/phyllite from this and the Cabo Ortegal Complex yield plateau ages which range from 367 Ma to 295 Ma. Analyses of similar material from the relative autochthon yield plateau ages between 359 Ma and 275 Ma. Muscovite concentrates from three late- to post-kinematic granitic stocks yield plateau ages between 309 Ma and 274 Ma.

At least seven of the $^{40}Ar/^{39}Ar$ analyses from metamorphic rocks record variable thermal rejuvenation of intracrystalline argon systems associated with emplacement of proximal granitic stocks. The remaining analyses may be used to constrain the local age of various Variscan tectonothermal events. The oldest fabric ages are recorded in allochthonous units whereas the youngest fabric ages occur along the boundary between internal and external zones. Middle Devonian ages are recorded in the allochthon and suggest a chronological continuity with deformational events in the relative autochthon, where Variscan deformation initiated in the Upper Devonian and diachronously prograded eastward. The first deformational events recorded in the limit within the internal and external zones occurred ca. 20–25 Ma later (lower Namurian). Variscan deformation systematically prograded diachronously eastward across the orogen as new crustal material was added along the front of the developing orogenic wedge. However, the entire orogen remained tectonically active with different structural features forming at different times and at different places. An average propagation rate of ca. 5 km/m.y. is suggested by consideration of a 20–25 Ma difference in correlative fabric ages and present separations.

Keywords: absolute age, $^{40}Ar/^{39}Ar$; fabric; Iberian Peninsula; Variscides

1. Introduction

The Iberian Massif comprises the westernmost exposures of the European Variscan orogen. Its internal tectonic zonation can be correlated with that of the rest of the Variscan massifs (Fig. 1), and the NW sectors include far-traveled allochthonous terranes of variable provenance and origin (Arenas et al., 1986).

Structurally underlying the Iberian allochthonous complexes are several lithotectonic zones (Fig. 2) which have been considered to represent an Iberian relative autochthon (Ribeiro et al., 1990), even though they have been affected by significant tectonic displacements. All initiated along the continental margin of Gondwana, and do not record any significant pre-Variscan shortening. Most of these zones are presently part of the Variscan 'internides'. Only the Iberian Cantabrian Zone displays characteristics of orogenic 'externides'.

The width of the NW sections of the massif (ca. 400 km) combined with the extent of prior resolution of its tectonothermal evolution make this area an ideal location to evaluate the duration of the orogenic process and to resolve potential diachronism of deformational events through coordinated geochronological and structural studies.

Syn- and post-orogenic sedimentary sequences permit paleontological dating of deformational events in the Cantabrian Zone only. Numerous isotopic ages have been reported for the various Iberian Variscan granitoids, but few have been available to constrain the relative chronology of deformational fabrics (exceptions include some of the allochthonous terranes). Although some of the granite ages broadly constrain the ages of late deformational phases, the precise age of earlier and more regionally penetrative phases has been largely unknown throughout most of NW Iberia.

To more precisely constrain the timing of the main tectonothermal events, the main deformation fabrics were sampled along a systematic traverse across the various tectonic zones and units, and multigrain concentrates of hornblende and muscovite together with whole-rock slate/phyllite samples were dated using $^{40}Ar/^{39}Ar$ incremental-release methods.

The interpretation of these results depends on relationships between the thermal and deformational histories and the closure of the isotope systems. Therefore, X-ray diffraction and electron microprobe analyses were carried out to help constrain the temperatures represented by the fabrics.

2. Geology of the study area and previous geochronology

The geological evolution of the NW Iberian Massif has been previously described in detail, and comprehensive contributions have summarized structural characteristics (e.g., Díez Balda et al., 1990; Martínez Catalán et al., 1990, 1996; Ribeiro et al., 1990; Pérez-Estaún et al., 1991), metamorphism (Arenas et al., 1986; Martínez and Rolet, 1988; Gil Ibarguchi and Arenas, 1990) and magmatism (Bellido Mulas et al., 1987; Corretgé et al., 1990). The area essentially represents a collisional belt in which dismembered ophiolitic units are interpreted to mark a suture. One of the colliding elements was Paleozoic Gondwana (based on faunistic and stratigraphic correlation: Paris and Robardet, 1977; Blaise and Bouyx, 1980; Martínez Catalán, 1990). The other element included an accretionary prism which entrained tectonic units of oceanic crust and crustal elements of problematic origins (Martínez Catalán et al., 1996).

The study area comprises a complete section from various types of allochthonous structural units, included in the Galicia-Trás-os-Montes Zone (GTMZ; Farias et al., 1987) in the axial zone of the orogen, to the Cantabrian Zone (CZ) which is exposed in external sectors and forms the Asturian Arc (innermost part of the Ibero-Armorican Arc). The latter, together with the West Asturian–Leonese Zone (WALZ), the Central Iberian Zone (CIZ), and the schistose domain of the GTMZ, comprise the Iberian relative autochthon (Figs. 1 and 2). The lithological associations, structures and fabrics of these different zones will be briefly described, together with the previous geochronological data. The time-scale calibration of Cowie and Basset (1989) will be used in the following description and the rest of the study. A summary of the available data is given in Fig. 3.

2.1. Galicia-Trás-os-Montes Zone (GTMZ)

The Galicia-Trás-os-Montes Zone is an internally imbricated ensemble composed of two contrasting

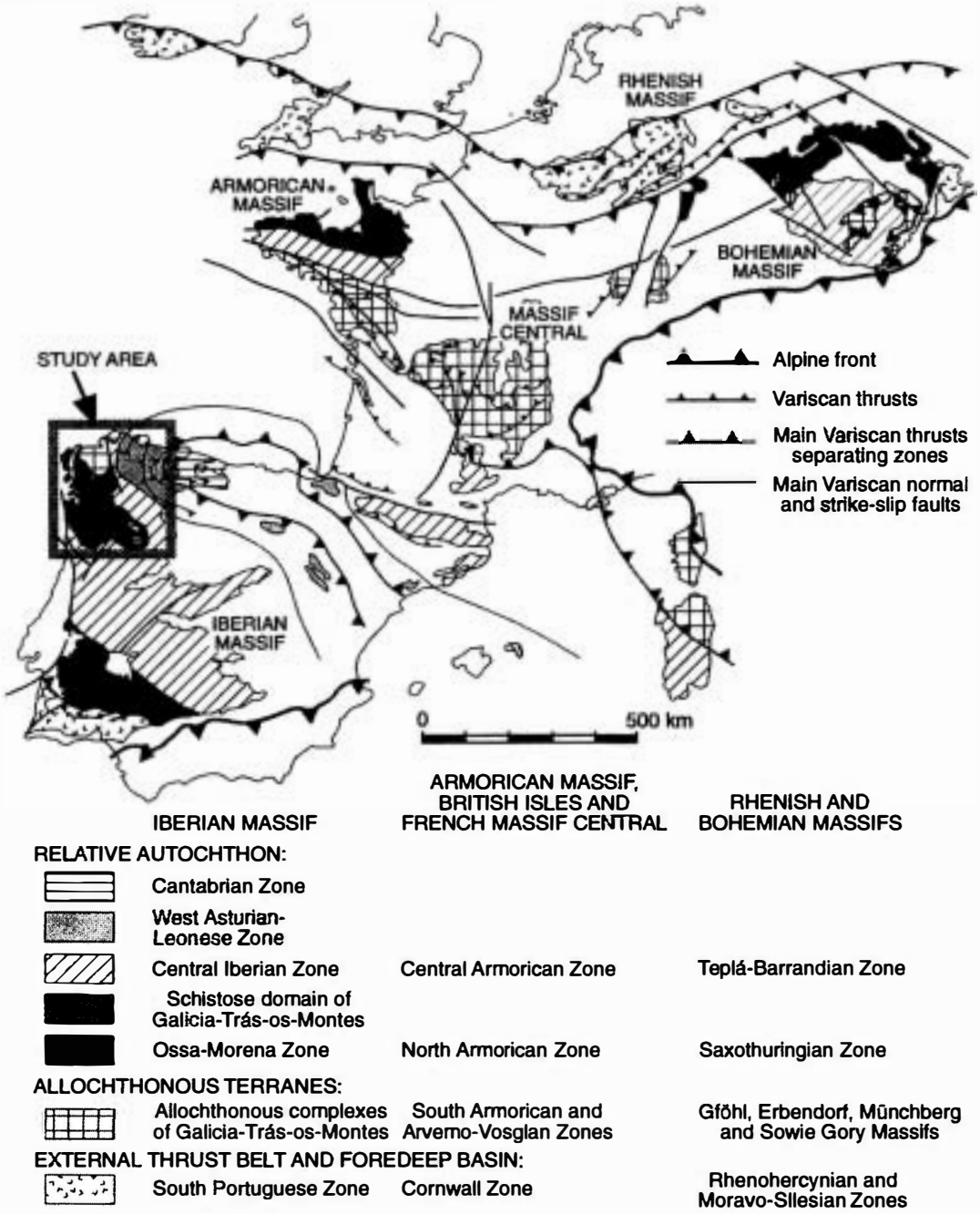

Fig. 1. Generalized geological map of the European Variscan orogen showing the location of the study area. After Martínez Catalán (1990), and mainly based on Julivert et al. (1972), Autran and Cogné (1980) and Tollman (1982).

tectonic elements (Fig. 2): (1) a domain of largely allochthonous crystalline nappe complexes with mafic and related rocks; and, (2) a schistose domain, consisting essentially of metasedimentary and volcanic rocks (Farias et al., 1987). The stratigraphic characteristics and tectonometamorphic evolution of the

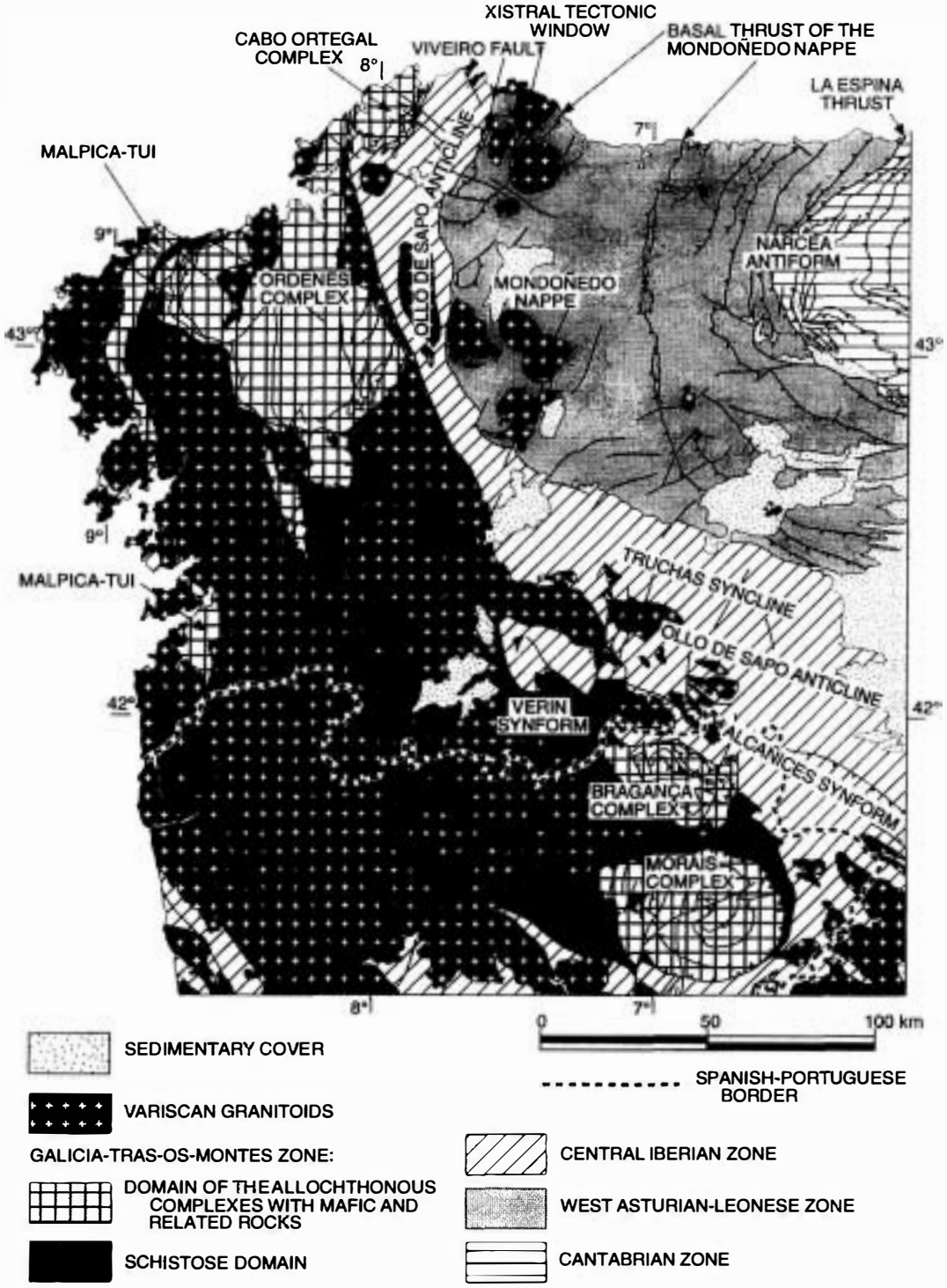

Fig. 2. Generalized geological map of the study area outlining the different zones of the NW Iberian Massif and the main structural elements.

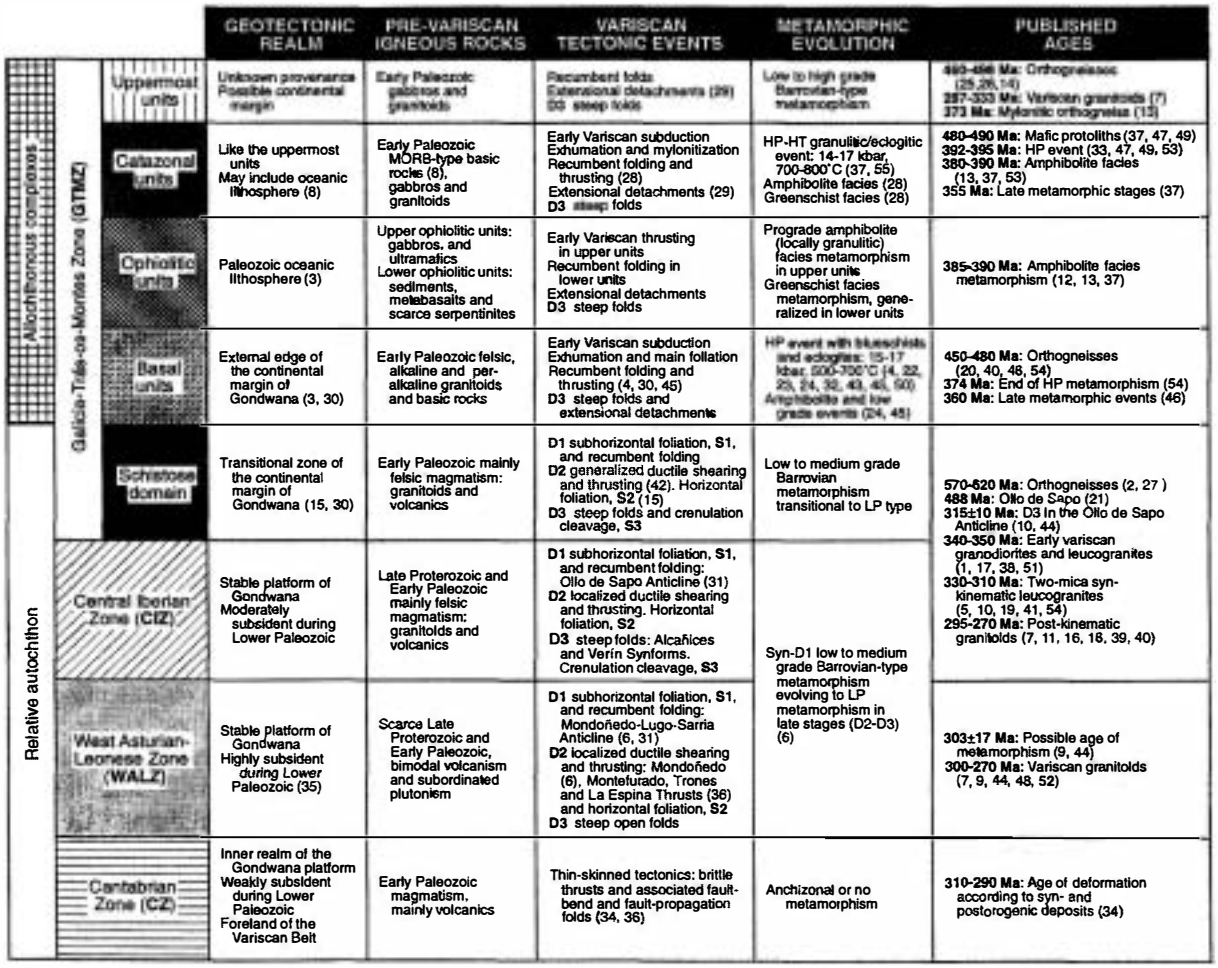

Fig. 3. Summary of geological information available for the different zones and units, arranged in their relative stacking position, from more-internal units (top) to external zones (bottom). Patterns in the columns to the left correspond to those used in Figs. 1, 2, 4 and 5. Numbers between brackets correspond to: 1 = Abranches et al. (1979); 2 = Allegret and Iglesias Ponce de León (1987); 3 = Arenas et al. (1986); 4 = Arenas et al. (1995); 5 = Barr and Areias (1980); 6 = Bastida et al. (1986); 7 = Bellido et al. (1992); 8 = Bernard-Griffiths et al. (1985); 9 = Capdevila and Vialette (1965); 10 = Capdevila and Vialette (1970); 11 = Cocherie (1978); 12 = Dallmeyer and Gil Ibarguchi (1990); 13 = Dallmeyer et al. (1991); 14 = Dallmeyer and Tucker (1993); 15 = Farias et al. (1987); 16 = Fourcade et al. (1989); 17 = Gallastegui (1993); 18 = García Garzón (1987); 19 = García Garzón and Locutura (1981); 20 = García Garzón et al. (1981); 21 = Gebauer (1993); 22 = Gil Ibarguchi (1995); 23 = Gil Ibarguchi and Dallmeyer (1991); 24 = Gil Ibarguchi and Ortega Gironés (1985); 25 = Kuijper (1979); 26 = Kuijper (1980); 27 = Lancelot et al. (1985); 28 = Marcos et al. (1984); 29 = Martínez Catalán and Arenas (1992); 30 = Martínez Catalán et al. (1996); 31 = Matte (1968); 32 = Munhá et al. (1984); 33 = Ordóñez Casado et al. (1996); 34 = Pérez-Estaún et al. (1988); 35 = Pérez-Estaún et al. (1990); 36 = Pérez-Estaún et al. (1991); 37 = Peucat et al. (1990); 38 = Pinto (1984); 39 = Priem et al. (1965); 40 = Priem et al. (1970); 41 = Priem and Den Tex (1984); 42 = Ribeiro (1974); 43 = Ribeiro (1976); 44 = Ries (1979); 45 = Rubio Pascual et al. (1993); 46 = Santos Zalduegui et al. (1995); 47 = Santos Zalduegui et al. (1996a); 48 = Santos Zalduegui et al. (1996b); 49 = Schäfer et al. (1993); 50 = Schermerhorn and Kotsch (1984); 51 = Serrano Pinto et al. (1987); 52 = Suárez et al. (1978); 53 = Valverde Vaquero and Fernández (1996); 54 = Van Calsteren et al. (1979); 55 = Vogel (1967).

latter suggest a close affinity with the underlying zones and, for this reason, the schistose domain has been considered as part of the relative autochthon.

2.1.1. Allochthonous complexes

Allochthonous crystalline nappe complexes are presently exposed within structural synforms formed

during the late stages of Variscan orogenesis. These include the Malpica–Tui, Ordenes, Cabo Ortegal, Bragança and Morais complexes (Fig. 2). They consist of allochthonous structural units of diverse provenance and with different tectonothermal histories. Traced structurally downward these include uppermost, catazonal, ophiolitic and basal tectonic units (Figs. 3–5). Several of these units are generally exposed in each complex (except for Malpica–Tui, where only basal units are preserved).

Uppermost units consist of terrigenous sedimentary rocks, amphibolites, and Lower Ordovician gabbros and augengneisses (see Fig. 3 and references therein). In the Ordenes Complex, metamorphism ranges from low-grade (chlorite zone) in uppermost tectonostratigraphic levels, to high-grade (sillimanite–K-feldspar zone) below. The limits between different metamorphic zones are often marked by extensional faults (Díaz García, 1990). One of these, the Corredoiras Detachment (Fig. 5), separates uppermost units from underlying catazonal units (Martínez Catalán and Arenas, 1992).

Catazonal units include paragneisses, mafic and ultramafic rocks. MORB-type igneous rocks have been described by Bernard-Griffiths et al. (1985), but the abundance of sedimentary rocks in these and uppermost units suggests either an arc-related environment (Arenas et al., 1986; Peucat et al., 1990) or a rifted continental margin setting. The metamorphic evolution included an initial high-pressure/high-temperature (HP–HT) granulitic/eclogitic event (Vogel, 1967) followed by a penetrative mylonitization in the amphibolite facies. The amphibolitic foliation was deformed by recumbent folding and subsequent thrusting under greenschist-facies conditions (Marcos et al., 1984). Isotopic data (Fig. 3) include Early Ordovician protolith ages, an Early Devonian age for the HP metamorphism, related to an early Variscan subduction, an Early–Middle Devonian age for the amphibolite-facies mylonitization and a Late Devonian–Early Carboniferous age for the final metamorphic stages.

Ophiolitic units are considered to mark the suture of an early Variscan crustal collision. Units in amphibolite facies, locally granulite facies (Díaz García, 1990), occupy uppermost tectonostratigraphic positions. These comprise medium- to coarse-grained metagabbros and ultramafics. They are structurally underlain by greenschist-facies ophiolitic rocks consisting of metabasites, metapelites, and small, isolated bodies of serpentinite. They have been affected by east-vergent, recumbent folding with development of penetrative mylonitic fabrics. Prograde recrystallization under amphibolite-facies conditions has been dated as Early Devonian (Fig. 3).

Basal units consist of schists and paragneisses, felsic and biotitic orthogneisses, alkaline and peralkaline orthogneisses, eclogites and amphibolites. Palynological characteristics suggest a middle to Late Ordovician age for the upper sedimentary sequences exposed in the Malpica–Tui Complex (Fombella Blanco, 1984). The orthogneisses have yielded Ordovician isotopic ages (Fig. 3). The amphibolites are intercalated with metasedimentary rocks and orthogneisses. This bimodal magmatism and the presence of per-alkaline rocks suggests that the units originated within a passive continental margin that evolved during Ordovician rifting (Arenas et al., 1986). Because they structurally underlie ophiolites, these units are interpreted to represent distal parts of the Gondwana continental margin.

The presence of blueschists, eclogites and, locally, jadeite (references in Fig. 3) records an initial episode of high-pressure (HP) metamorphism related to subduction. The high-pressure episode was followed by marked (from 15 to 7 kbar) and rapid decompression which was nearly isothermal (Arenas et al., 1995) and accompanied formation of a regional foliation. Abundant extensional detachments indicate that tectonic denudation was responsible for much of the decompression. They appear to have alternated in time with development of east-vergent recumbent folds and thrust faults. This has been attributed to attempted subsequent underthrusting of continental crust, which triggered a buoyant as-

Fig. 4. Geological map of the study area (based on Parga Pondal et al., 1982), modified and outlining: (1) the various types of allochthonous tectonic units; (2) the main stratigraphic ensembles in the Iberian relative autochthon; and (3) the main granitic groups. $^{40}Ar/^{39}Ar$ sample locations and obtained ages are shown. Also included are locations of the cross-sections of Fig. 5.

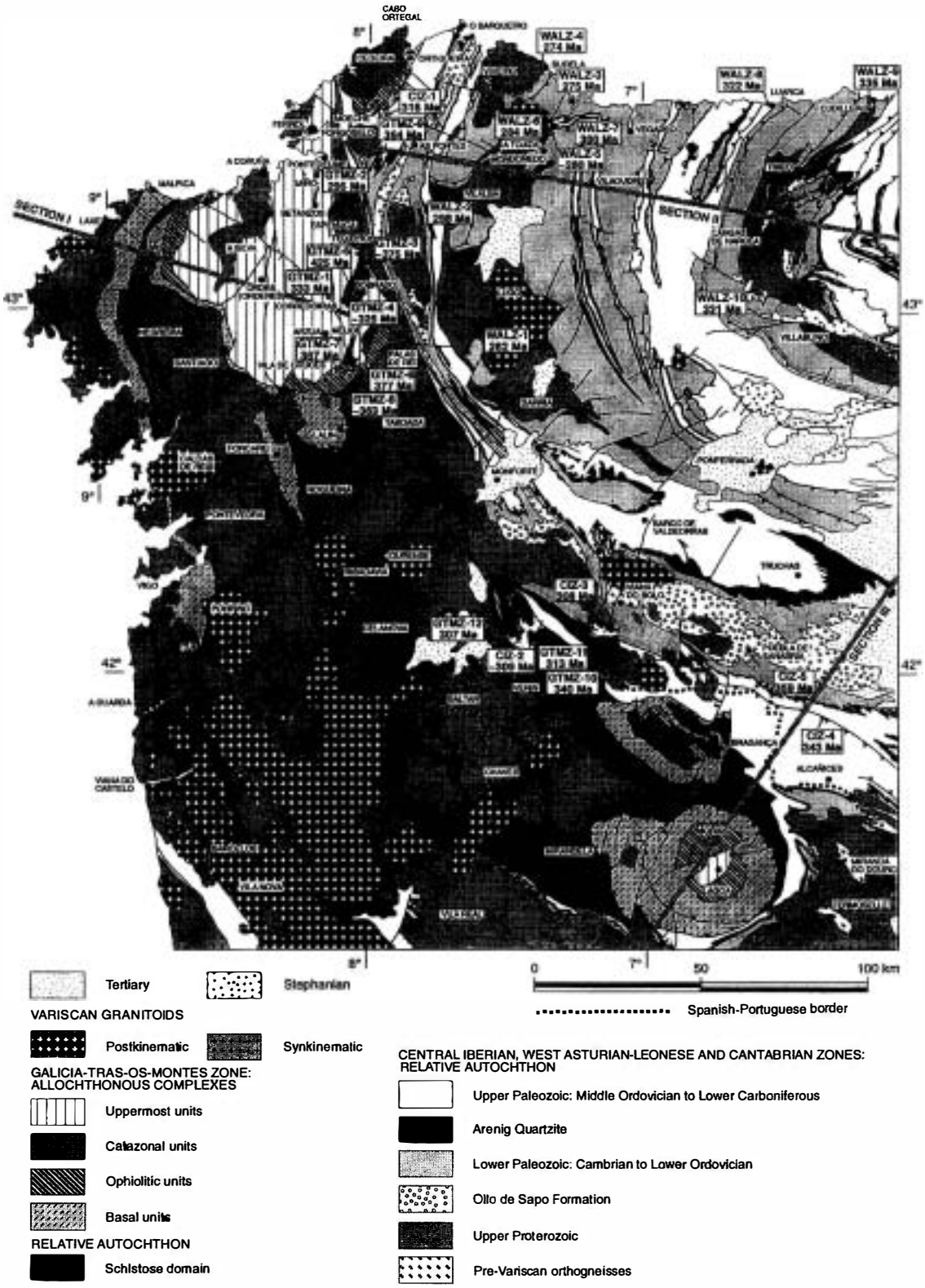
CABO ORTEGAL
O BARQUEIRO
WALZ-4 374 Ma
WALZ-3 375 Ma
WALZ-8 332 Ma
WALZ-9 336 Ma
CIZ-1 316 Ma
OTMZ-6 384 Ma
WALZ-6 394 Ma
WALZ-7 391 Ma
WALZ-5 386 Ma
A CORUÑA
MALPICA
SECTION I
OTMZ-2 395 Ma
OTMZ-3 -372 Ma
OTMZ 405 Ma
OTMZ-1 -392 Ma
OTMZ-4 -388 Ma
OTMZ-7 -387 Ma
OTMZ -377 Ma
OTMZ-8 -369 Ma
WALZ-2 -388 Ma
SECTION II
WALZ-10 321 Ma
WALZ-1 -382 Ma
PONFERRADA
BARCO DE VALDEORRAS
VIGO
CIZ-3 -388 Ma
OTMZ-13 -397 Ma
CIZ-2 -388 Ma
OTMZ-1 -313 Ma
OTMZ-10 -340 Ma
A GUARDA
CIZ-4 343 Ma
ALCAÑICES
VILA DO CASTELO
MIRANDA DO DOURO
Tertiary
Stephanian
VARISCAN GRANITOIDS
Postkinematic
Synkinematic
GALICIA-TRAS-OS-MONTES ZONE: ALLOCHTHONOUS COMPLEXES
Uppermost units
Catazonal units
Ophiolitic units
Basal units
RELATIVE AUTOCHTHON
Schistose domain
CENTRAL IBERIAN, WEST ASTURIAN-LEONESE AND CANTABRIAN ZONES: RELATIVE AUTOCHTHON
Upper Paleozoic: Middle Ordovician to Lower Carboniferous
Arenig Quartzite
Lower Paleozoic: Cambrian to Lower Ordovician
Ollo de Sapo Formation
Upper Proterozoic
Pre-Variscan orthogneisses
0
50
100 km
Spanish-Portuguese border

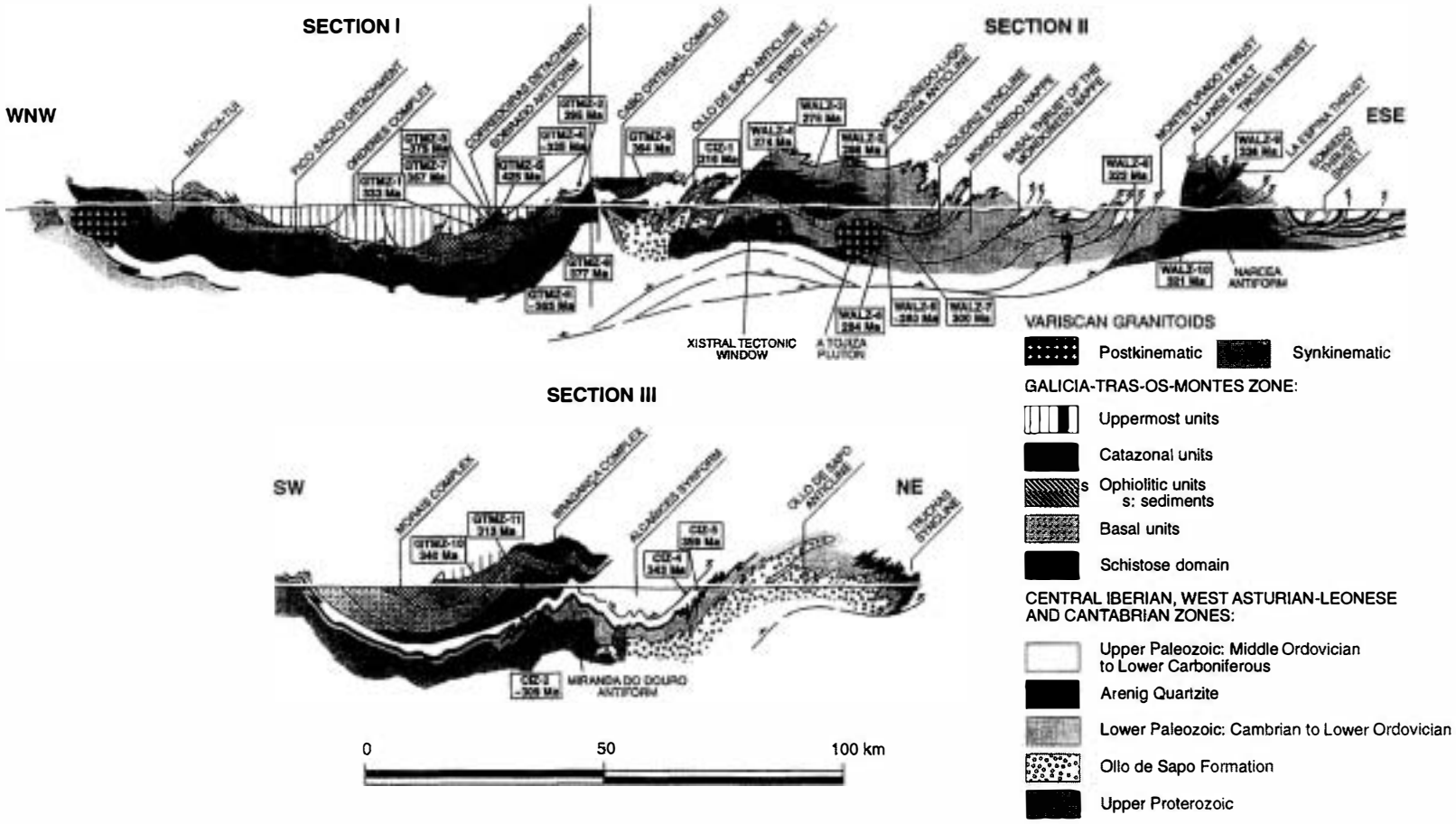

Fig. 5. Generalized geological cross-sections illustrating the main structures and their denomination. For location, see Fig. 4. Sections I and II are connected to provide a comprehensive view of the structure of the entire study area. Most of the dated samples have been projected along-strike into the sections, and the $^{40}Ar/^{39}Ar$ ages are included. Ages preceded by '~' represent possible approximate ages for spectra not defining a plateau, but which, for several contiguous temperature increments, record apparent ages restricted to a relatively narrow range. The depth interpretation of the Central Iberian and West Asturian–Leonese zones is based on the seismic profile ESCI-N3.3 (Martínez Catalán et al., 1995).

cent and exhumation of the allochthonous crystalline complexes (Martínez Catalán et al., 1996). The generalized eastward vergence of structures developed in the NW Iberian Massif is considered to reflect the polarity of subduction. Final deformational stages have been dated as Middle–Late Devonian and the decompressive episode took place in a ca. 10–15 m.y. time span (Fig. 3).

2.1.2. Schistose domain

A several kilometers thick sequence (Fig. 5) structurally underlies most of the allochthonous complexes (Ribeiro, 1974; Farias et al., 1987). It consists of schists, often carbonaceous, occasional quartzites and felsic igneous rocks, both volcanic and plutonic. Amphibolites occur locally. Depositional ages are Paleozoic, and the overall stratigraphy displays similarities with both the basal units of the allochthonous complexes and the autochthonous sequences.

The tectonometamorphic evolution included an initial, intermediate-pressure, Barrovian-type episode, followed by a low-pressure episode with variable temperatures. Three main compressional deformation phases have been described: D_1 produced a regional penetrative tectonic foliation (S_1) and is locally associated with recumbent folding. D_2 gave rise to a foliation (S_2) which was originally subhorizontal and related to the thrusting of the structurally overlying allochthonous crystalline complexes (Marquínez García, 1984) and of the domain itself onto the CIZ. D_3 locally folded previous structures and led to formation of regional steep synforms and antiforms with axial planar crenulation cleavages (S_3). The folds were locally contemporary with formation of transcurrent, subvertical shear zones.

The stratigraphic, structural and metamorphic similarities of the schistose domain with the underlying CIZ suggest a palinspastic proximity between both, and a relative small displacement along the thrust separating them. These characteristics suggest that this domain, also termed a 'parautochthon' (Ribeiro et al., 1990), should be considered part of the relative autochthon.

2.2. Central Iberian Zone (CIZ)

In the western and southern parts of the study area, the CIZ consists of a terrigenous Upper Proterozoic sequence which includes volcanic rocks and granitic orthogneisses, which are unconformably overlain by shallow-water, marine, Lower Ordovician sedimentary rocks. The pre-orogenic succession may be traced stratigraphically upward into a shallow-water, Silurian–Lower Devonian platform facies. In the Alcañices Synform (Figs. 2 and 5), a Devonian–Lower Carboniferous flysch (San Vitero Fm.) occurs in the upper parts of the sequence. This synorogenic deposit has not been precisely dated. It was deformed by the first regional deformation phase, but includes metamorphic pebbles of Variscan origin (Ribeiro, 1974; Quiroga, 1982). In the east and northeast of the study area, an augengneiss, of subvolcanic to volcaniclastic origin dated as Early Ordovician (Ollo de Sapo Fm.) underlies the Paleozoic sediments (Parga Pondal et al., 1964).

The metamorphic evolution was similar to that of the schistose domain. D_1 was associated with recumbent, east-vergent folding. The Ollo de Sapo Anticline is the largest of these structures (Figs. 2, 4 and 5). A penetrative slaty cleavage (S_1) developed in all pelitic lithologies. The main D_2 thrust is represented by the lower tectonic contact of the schistose domain (Fig. 5). Also, several thrusts have been mapped in the Alcañices Synform (Vacas and Martínez Catalán, 1987; Antona and Martínez Catalán, 1990). These appear to merge into a sole thrust connected with the basal thrust of the schistose domain. Penetrative S_2 cleavages and phyllonites developed proximal to the thrust faults. D_3 folded the D_1 recumbent structures and D_2 thrusts producing large, open structures such as the Alcañices Synform and the Miranda do Douro Antiform (Figs. 2 and 5). The age of this event in the Ollo de Sapo Anticline has been dated at 315 ± 10 Ma (Fig. 3).

2.3. West Asturian–Leonese Zone (WALZ)

This zone represents the easternmost internal zone of the Iberian Massif. It is characterized by an extensive preorogenic Paleozoic sequence (5000–10,000 m thick). The WALZ was more subsident than adjacent zones during the prolonged phase of extensional tectonics related to evolution along the Gondwana stable margin (Pérez-Estaún et al., 1990; Liñán and Quesada, 1990; Martínez Catalán et al., 1992).

The tectonothermal evolution is similar to that of

the CIZ. D_1 is characterized by recumbent folds, the largest being the Mondoñedo–Lugo–Sarria Anticline (Matte, 1968) and the Vilaoudriz Syncline (Fig. 5). D_2 produced thrusts and associated ductile shear zones with S_2 cleavage. The Mondoñedo Nappe, in the west, displays tectonic transport of at least 40 km (Bastida et al., 1986). More eastern thrusts have been interpreted to merge at depth with a sole thrust (Pérez-Estaún et al., 1991; Martínez Catalán et al., 1995). La Espina and Trones thrusts mark the tectonic separation between the WALZ and the CZ (Gutiérrez-Alonso, 1996; Gutiérrez-Alonso and Nieto, 1996). Subvertical D_3 folds and S_3 crenulation cleavage are also common; for instance, in the area around Luarca (Pulgar, 1980, 1981).

2.4. Cantabrian Zone (CZ)

This zone represents the foreland thrust belt of the Variscan orogen. The stratigraphic succession is generally non-metamorphic. It consists of a pre-orogenic, pre-Carboniferous sequence and a synorogenic, mainly paralic Carboniferous sequence (Marcos and Pulgar, 1982) with characteristics of a synorogenic molasse. The overall structure of the CZ is thin-skinned, and the thrusts propagated forward and systematically migrated eastward with time. Cleavage development is only local and, often, displays no relationship to compressional structures (Aller et al., 1987).

Deformational ages in the CZ are constrained by paleontological dating of syn- and post-orogenic deposits. The Somiedo Thrust Sheet, the westernmost of the Cantabrian units, was emplaced during the early Westphalian. More external structures originated during the Kasimovian (i.e., lower Stephanian; Pérez-Estaún et al., 1988). This implies a time span of ca. 15–20 m.y. for the emplacement of the units.

2.5. Variscan granitoids

Numerous granitic stocks were emplaced during phases of the Variscan tectonothermal evolution. These are most abundant in more-internal zones and decrease eastward. They are scarce in the eastern parts of the WALZ and rare in the CZ. Granitic activity included syn- and post-kinematic phases (Bellido Mulas et al., 1987). Syn-kinematic granitoids include meta-aluminous biotite granites and granodiorites, per-aluminous two-mica granites and adamellites and several types of inhomogeneous granitoids. All were emplaced after D_1 and, generally, also after D_2 (with the exception of a few massifs in the Mondoñedo Nappe which were deformed at its basal shear zone; Martínez Catalán, 1983). Most syn-kinematic granitoids were deformed by D_3.

Available isotopic ages have been included in Fig. 3, together with their references. In the allochthonous complexes, granite emplacement occurred in the Carboniferous, beginning in the late Visean. In the schistose domain and the CIZ, the oldest syn-kinematic massifs were emplaced in the Tournaisian. Younger massifs, still syn-kinematic, intruded during the Visean–Namurian, and post-kinematic ones during the Stephanian–Permian. In the WALZ, published ages for syn-kinematic granites are as young as Stephanian, and post-kinematic massifs range from the same age to Early Permian.

3. Analytical methods

3.1. $^{40}Ar/^{39}Ar$

The mineral concentrates and whole-rock samples were analyzed using incremental-release $^{40}Ar/^{39}Ar$ analysis. The techniques used generally followed those described by Dallmeyer and Gil Ibarguchi (1990). They were irradiated for 40 h at the USGS TRIGA Reactor, Denver. Variations in flux of neutrons along the length of the irradiation assembly were monitored with several mineral standards, including MMhb-1 (Sampson and Alexander, 1987). The samples were incrementally heated until fusion in a double-vacuum, resistance-heated furnace. Temperatures were monitored with a direct-contact thermocouple. Total-system blanks were periodically measured across the entire temperature range of the analyses. Beam intensities were measured using a Faraday collector. Intralaboratory uncertainties have been calculated by statistical propagation of uncertainties associated with measurements of each isotopic ratio (at two standard deviations of the mean) through the age equation. Interlaboratory uncertainties are ca. ±1.25–1.5% of the quoted age. A 'plateau' is considered defined if the ages recorded by four or more contiguous gas fractions

(with similar apparent K/Ca ratios) each representing >4% of the total ^{39}Ar evolved (and together constituting >50% of the total ^{39}Ar evolved) are mutually similar within ±1% intralaboratory uncertainty. Analyses of the MMhb-1 monitor show that apparent K/Ca ratios may be calculated through the relationship $0.518\ (+0.005) \times (^{39}Ar/^{37}Ar)_{corrected}$. Plateau portions of the analyses have been plotted on $^{36}Ar/^{40}Ar$ vs. $^{39}Ar/^{40}Ar$ isotope correlation diagrams. Regression techniques followed methods described by York (1969). A mean square of the weighted deviates (MSWD) has been used to evaluate the isotopic correlations. Any MSWD value greater than 2.5 was considered to indicate that no reliable line was defined.

3.2. X-ray diffraction

Whole-rock samples of relatively low-grade slate/phyllite have been analyzed in several areas. In view of their relatively low-grade and polymineralic character, it was considered critical to quantify the metamorphic state in order to permit resolution of the effects of detrital vs. authigenic white mica. Previous calibration of low- and very low-grade terrains and evaluation of the control of metamorphic rejuvenation of low-grade slate/phyllite has been possible through determination of quartz-normalized illite crystallinity (e.g., Reuter, 1985; Dallmeyer and Takasu, 1992). With this purpose, seven representative Iberian whole-rock samples were selected for crystallinity analysis. Samples were disaggregated in a shatter box for 20 s. Bulk <2 μm-size fractions were isolated by differential settling in Atterberg cylinders and by centrifugation, following techniques listed in Reuter (1985). Illite crystallinity of these fractions was determined from oriented sedimentation slides by comparison of the {001} illite and {100} quartz (internal standard) reflections following the methods of Weber (1972). Cross-calibration suggests that the following values are appropriate for the equipment settings employed (compared with the calibrations of Teichmüller et al., 1979): greenschist/upper anchizone = 125; upper anchizone/middle anchizone = 205–210; middle anchizone/lower anchizone = 300; anchizone/diagenesis = 400.

3.3. Electron microprobe

Minerals of the samples studied were analyzed on thin-section and from the concentrates used for dating purposes. Analyses were performed using a Camebax-Microbeam microprobe at the University of Clermont-Ferrand. Operating conditions were 10 s counting time, ca. 10 nA beam current, and 15 kV accelerating voltage. Calibration was against BRGM (French Geological Survey) standard minerals, and the ZAF correction procedure was used. Fe^{3+} in amphibole, garnet, muscovite and biotite was calculated by charge balance and regression methods (cf. De Bruiyn et al., 1983; Droop, 1987; Holland and Blundy, 1994).

Temperature and pressure conditions of recrystallization were estimated using published formulations for thermobarometers of interest and the composition of coexistent minerals. The plagioclase–amphibole (Holland and Blundy, 1994) geothermometer, and the geobarometers of Raase (1974) and Brown (1977) were used on mafic rocks. Plagioclase–muscovite (Green and Usdansky, 1986), biotite–muscovite (Hoisch, 1989) and garnet–biotite (Perchuk, 1991) geothermometers, and the Si content in muscovite (Massone and Schreyer, 1987) and garnet–biotite–muscovite–plagioclase–quartz (Hoisch, 1990) geobarometers were used on acid rocks and metapelites. Results are average values, with standard deviation expressed as ±.

4. Sample description

$^{40}Ar/^{39}Ar$ analyses of 27 representative samples collected from structural units exposed in the northwestern sectors of the Variscan Iberian Massif are presented. These include twelve samples from the GTMZ, five samples from the CIZ and ten samples from the WALZ. Sample localities and relative structural positions are shown in Figs. 4 and 5. Table 1 lists the rock types and corresponding units and summarizes the thermobarometric and $^{40}Ar/^{39}Ar$ results. The coordinates of the sample localities are listed in Table 2.

GTMZ-1 and GTMZ-2 are phyllite samples collected within the uppermost unit in the Ordenes Complex. A regional foliation, initially subhorizon-

Table 1
Summary of the $^{40}Ar/^{39}Ar$ analytical data for incremental-heating experiments

Sample	Rock type	Structural unit	Thermobarometric information	Type of analysis	Apparent total gas age (Ma)	Total gas fractions	Plateau age (Ma)	Plateau gas fractions	% ^{39}Ar of total in plateau	Isotope-correlation age (Ma)	Preferred age (Ma)
GTMZ-1	Phyllite	Uppermost unit, Ordenes Complex	Chlorite zone, greenschists	Whole-rock	316.5 ± 0.3	12	333.3 ± 0.3	6	58.30		333.3 ± 0.3
GTMZ-2	Phyllite	Uppermost unit, Ordenes Complex	Biotite zone, greenschists	Whole-rock	284.2 ± 0.3	12	294.7 ± 0.2	9	82.40		294.7 ± 0.2
GTMZ-3	Amphibolite	Uppermost unit, Ordenes Complex	T: 600 ± 45°C for P = 5 kbar	Hornblende	375.8 ± 2.1	16					~375
GTMZ-4	Paragneiss	Catazonal unit, Ordenes Complex	Retrograded to greenschists facies	Muscovite	318.1 ± 0.5	9					~325
GTMZ-5	Amphibolite	Catazonal unit, Ordenes Complex	Amphibolite facies	Hornblende	433.7 ± 1.2	13	432.1 ± 1.1	10	93.53	425.2 ± 1.2	425.2 ± 1.2
GTMZ-6	Amphibolite	Ophiolitic unit, Ordenes Complex	T: 600 ± 45°C, P > 5 kbar	Hornblende	381.3 ± 1.0	14	378.1 ± 0.4	9	91.37	376.8 ± 0.4	376.8 ± 0.4
GTMZ-7	Metapelite	Ophiolitic unit, Ordenes Complex	Low-T greenschists facies	Muscovite	360.3 ± 0.4	13	366.8 ± 0.4	11	95.09		366.8 ± 0.4
GTMZ-8	Metapelite	Ophiolitic unit, Ordenes Complex	Low-T chlorite zone	Muscovite	344.7 ± 0.4	13					~363
GTMZ-9	Metapelite	Ophiolitic unit, Cabo Ortegal Complex	T < 400°C	Whole-rock	357.0 ± 0.8	16	364.4 ± 0.7	7	65.60		364.4 ± 0.7
GTMZ-10	Phyllite	Schistose domain, Verín Synform	T < 400°C, upper anchizone	Whole-rock	308.3 ± 1.0	12	340.0 ± 0.9	4	51.41		340.0 ± 0.9
GTMZ-11	Phyllonite	Schistose domain, Verín Synform	Upper anchizone/greenschists	Whole-rock	307.6 ± 0.7	17	313.3 ± 0.6	9	57.29		313.3 ± 0.6
GTMZ-12	Quartzite	Schistose domain, Verín Synform	400°C<T<650°C for P = 5 kbar	Muscovite	307.1 ± 0.6	9	307.0 ± 0.6	8	98.93		307.0 ± 0.6
CIZ-1	Metavolcanite	Ollo de Sapo A.	T: 355 ± 10°C for P_{max} = 5 kbar	Muscovite	314.6 ± 1.4	13	316.4 ± 0.9	8	87.10		316.4 ± 0.9
CIZ-2	Slate	Verín Synform	Upper anchizone	Whole-rock,	309.4 ± 1.0	16					~309
CIZ-3	Granite	Verín Synform	T: 695 ± 35°C for P = 2 kbar	Muscovite	308.1 ± 0.7	9	308.5 ± 0.6	7	91.84		308.5 ± 0.6
CIZ-4	Phyllite	Alcañices Synform	Middle anchizone	Whole-rock	339.8 ± 0.4	10	342.6 ± 0.3	5	70.71		342.6 ± 0.3
CIZ-5	Slate	Alcañices Synform	Middle anchizone	Whole-rock	346.2 ± 0.2	10	359.3 ± 0.2	5	68.11		359.3 ± 0.2
WALZ-1	Granite	Mondoñedo Nappe	T: 500–700°C, P: 4.5 ± 0.5 kbar	Muscovite	282.7 ± 1.0	14	282.2 ± 0.8	9	86.13		282.2 ± 0.8
WALZ-2	Schist	Mondoñedo Nappe	T: 575 ± 15°C, P: 6 ± 0.3 kbar	Muscovite	297.5 ± 0.9	15	298.2 ± 0.6	9	90.88		298.2 ± 0.6
WALZ-3	Phyllonite	Mondoñedo Nappe	T: 500 ± 30°C, P < 5 kbar	Muscovite	275.5 ± 1.1	15	275.5 ± 0.9	12	93.76		275.5 ± 0.9
WALZ-4	Granite	Xistral Tectonic Window	T: 625 ± 20°C	Muscovite	273.8 ± 0.8	9	274.1 ± 0.7	8	98.10		274.1 ± 0.7
WALZ-5	Schist	Mondoñedo Nappe	T: 555 ± 10°C for P_{max} = 2 kbar	Muscovite	281.3 ± 0.6	9					~280
WALZ-6	Granite	Mondoñedo Nappe	T: 540 ± 10°C, P < 2 kbar	Muscovite	283.2 ± 0.9	9	283.8 ± 0.7	7	96.05		283.8 ± 0.7
WALZ-7	Slate	Mondoñedo Nappe	T: 400 ± 20°C for P_{max} = 5 kbar	Whole-rock	291.6 ± 1.4	12	300.0 ± 1.0	9	88.15		300.0 ± 1.0
WALZ-8	Slate	Montefurado Thrust Sheet	T: 340 ± 10°C, upper anchizone	Whole-rock	320.9 ± 0.3	12	322.1 ± 0.2	6	76.54		322.1 ± 0.2
WALZ-9	Slate	La Espina Thrust Sheet	T: 300 ± 10°C, upper anchizone	Whole-rock	325.8 ± 0.3	11	336.5 ± 0.3	5	58.85		336.5 ± 0.3
WALZ-10	Phyllonite	Tronco Thrust Sheet	T: 300 ± 10°C for P < 5 kbar	Whole-rock	317.7 ± 1.2	16	321.1 ± 1.0	8	70.95		321.1 ± 1.0

Table 2
Coordinates of the sampling sites

Sample	Coordinates: Latitude	Longitude
GTMZ-1	43°1′59″N	8°9′17″W
GTMZ-2	43°21′9″N	8°11′47″W
GTMZ-3	43°8′23″N	8°2′10″W
GTMZ-4	43°2′10″N	8°2′19″W
GTMZ-5	43°2′2″N	8°3′43″W
GTMZ-6	42°50′10″N	8°1′20″W
GTMZ-7	42°49′27″N	8°7′23″W
GTMZ-8	42°48′30″N	8°4′34″W
GTMZ-9	43°33′21″N	7°58′10″W
GTMZ-10	41°57′13″N	7°22′54″W
GTMZ-11	42°5′16″N	7°25′9″W
GTMZ-12	42°8′58″N	7°35′0″W
CIZ-1	43°31′29″N	7°55′13″W
CIZ-2	42°7′35″N	7°27′56″W
CIZ-3	42°9′24″N	7°12′0″W
CIZ-4	41°52′0″N	6°21′49″W
CIZ-5	41°53′52″N	6°26′2″W
WALZ-1	42°48′57″N	7°29′53″W
WALZ-2	43°17′2″N	7°36′41″W
WALZ-3	43°38′34″N	7°20′18″W
WALZ-4	43°40′35″N	7°22′30″W
WALZ-5	43°28′47″N	7°20′13″W
WALZ-6	43°28′55″N	7°20′12″W
WALZ-7	43°29′28″N	7°17′0″W
WALZ-8	43°32′57″N	6°32′20″W
WALZ-9	43°34′3″N	6°8′57″W
WALZ-10	43°2′36″N	6°34′4″W

tal, was folded by steep, D_3 folds with an associated local development of crenulation cleavage.

GTMZ-3 is an amphibolite collected along the Corredoiras Detachment which separates uppermost from catazonal units (Fig. 5). The rock, originally a metagabbro, has been penetratively deformed and displays a fine-grained mylonitic foliation which developed during translation along the detachment.

GTMZ-4 and GTMZ-5 are, respectively, a paragneiss and an amphibolite from the catazonal unit exposed in the Sobrado Antiform (Fig. 5). Both have been retrogressed from high-pressure granulite facies and display mylonitic foliation which developed under decompressive conditions. Retrogression in the paragneiss was associated with greenschist-facies conditions.

GTMZ-6 to GTMZ-9 were collected in the ophiolitic units to date the main fabric developed in these units. Sample 6 is a garnet-bearing amphibolite from the upper ophiolitic units exposed in the eastern Ordenes Complex (Fig. 5). Samples 7 and 8 are metapelites from the lower greenschist-facies ophiolites in the eastern Ordenes Complex. Sample 9 is a similar metapelite from the Cabo Ortegal Complex.

GTMZ-10 and GTMZ-11 are a phyllite and a phyllonite collected within the schistose domain in the Verín Synform (Figs. 2 and 4). The former was collected to constrain the age of the regional foliation in this domain, and the latter to date the basal thrust separating the GTMZ and CIZ (Farias et al., 1987; Farias, 1990).

GTMZ-12 is a muscovite-rich quartzite from the schistose domain which occurred as a large xenolith in a syn-kinematic two-mica granite exposed west of the Verín Synform. Thermal effects are expected as a result of granite intrusion. It was collected to constrain the age of granite emplacement.

CIZ-1 and CIZ-2 represent samples collected in the Central Iberian autochthon immediately underlying the allochthonous units and schistose domain, respectively. Sample 1 is a mylonitic metavolcanite collected southeast of Cabo Ortegal. Sample 2 is a slate from the Verín Synform. They were chosen for analysis to constrain the ages of the subhorizontal fabrics.

CIZ-3 is from a syn-kinematic two-mica granite exposed east of the Verín Synform.

CIZ-4 and CIZ-5 are a phyllite and a slate from the Alcañices Synform (Figs. 2 and 5). Sample 4 was collected adjacent to the main D_2 thrust in the northeastern limb of the synform to control the age of regional thrusting. Sample 5 was collected to constrain the age of the regional S_1 cleavage developed in this area (normal limb of the Ollo de Sapo Anticline).

WALZ-1, WALZ-2 and WALZ-3 were selected to define the age of the S_2 foliation developed along the basal shear zone of the Mondoñedo Nappe. Sample 1 is a deformed two-mica granite from the Sarria pluton emplaced syn-kinematically with D_2. Sample 2 is a schist from within the shear zone. Sample 3 is a phyllonite from along the basal thrust exposed east of the Xistral Tectonic Window.

WALZ-4, WALZ-5 and WALZ-6 were collected to control the timing of late thermal events in the Mondoñedo Nappe. Sample 4 is a post-kinematic granitoid collected near the phyllonite sampled from

the basal thrust of the nappe. Sample 5 was collected in schists close to the contact with the post-kinematic A Tojiza pluton. Sample 6 is a granite collected near the border of this pluton.

WALZ-7, WALZ-8, and WALZ-9 are slates with penetrative S_1 cleavages collected eastward across the WALZ to date D_1. Sample 7 is from the Mondoñedo Nappe, near A Tojiza pluton. Sample 8 is from Luarca, an area were a penetrative S_3 cleavage is locally developed (Pulgar, 1981). Sample 9 was collected in Cudillero where the easternmost D_1 recumbent folds are exposed (Figs. 2 and 4).

WALZ-10 is a phyllonite collected in the basal shear zone of the Trones Thrust, near the limit between the internal and external zones. It was selected to constrain the local age of D_2 thrusting.

5. Results

Three multigrain concentrates of hornblende, twelve concentrates of muscovite, and twelve whole-rock samples were prepared from the representative samples. The $^{40}Ar/^{39}Ar$ analytical data are portrayed as age spectra in Figs. 6–8 and, together with the temperature estimates, summarized in Table 1. Additional tables listing all of the $^{40}Ar/^{39}Ar$ analytical data, the X-ray diffraction data for seven low-grade slates and phyllonites, and the mineral compositions from electron microprobe analyses are available and will be supplied upon request (address the correspondence to the second author). The preferred age for each sample has been included in the map and cross-sections (Figs. 4 and 5). For samples where no plateau or isotope correlation age is defined, an approximate reference age is suggested, based on the considerations discussed below.

5.1. Hornblende analyses

The three hornblende concentrates (Table 1) display internally discordant $^{40}Ar/^{39}Ar$ age spectra of variable complexity (Fig. 6). Apparent K/Ca ratios are relatively small and display little intrasample variation. All spectra are marked by considerable variations in apparent ages recorded by gas fractions evolved at low experimental temperatures. These are matched by fluctuations in apparent K/Ca ratios that suggest that experimental evolution occurred from compositionally distinct, relatively non-retentive phases. These could be represented by: (1) very minor, optically undetectable mineralogical contaminants in the hornblende concentrates; (2) petrographically unresolved exsolution or compositional zonation within constituent hornblende grains; (3) minor chloritic replacement of hornblende; and/or (4) intracrystalline inclusions.

5.1.1. GTMZ-3

The hornblende concentrate prepared from this sample displays an internally discordant release spectrum and does not define a plateau. No combinations of incremental data resulted in the definition of a meaningful isotope correlation. Therefore, no geologic significance is ascribed to the 375.8 ± 2.1 Ma total-gas age. However, the low- and intermediate-temperature increments suggest partial, post-crystallization thermal rejuvenation. The sample is a fine-grained nematoblastic amphibolite with a peak, syn-mylonitic mineral assemblage consisting of green hornblende, plagioclase (An_{20-35}), quartz, ilmenite and minor biotite. Some larger amphiboles with schiller-like microinclusions are probably derived from primary igneous pyroxenes of the original gabbro. Occasionally, diopsidic clinopyroxene has been preserved. Pressure of crystallization was probably not higher than 5 kbar in view of the Si, Al^{VI}, Na(M4) and Al^{IV} contents of amphibole (Raase, 1974, 1977). The temperature for recrystallization of amphibole, assuming equilibrium with plagioclase was around 600 ± 45°C for an assumed pressure of 5 kbar. Local development of sericite and clinozoisite from plagioclase, and of chlorite from amphibole, are retrogressive effects. Mylonitization along the Corredoiras Detachment occurred mainly in the amphibolite facies, but a final greenschist-facies paragenesis is locally developed. Assuming that the spectrum

Fig. 6. $^{40}Ar/^{39}Ar$ apparent age of amphibole and muscovite concentrates and whole-rock analyses from the Galicia-Trás-os-Montes Zone. Apparent K/Ca spectra are included for the hornblende and whole-rock analyses. Analytical uncertainties (2σ intralaboratory) are represented by vertical width of bars. Experimental temperatures increase from left to right. Plateau ages are listed where appropriate.

HORNBLENDE CONCENTRATES:

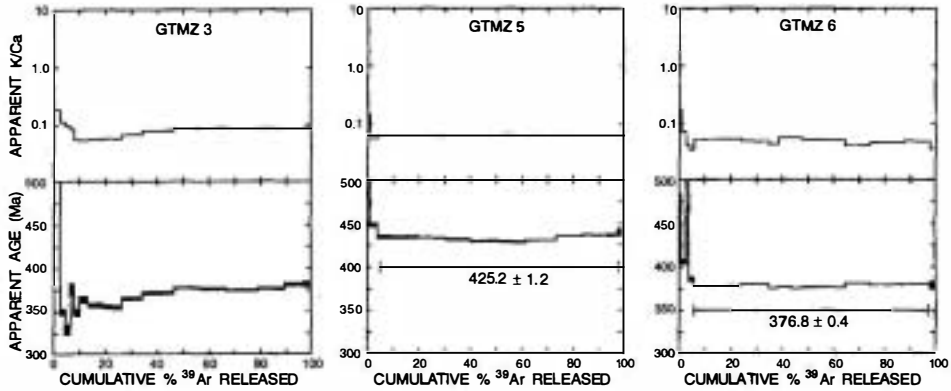

MUSCOVITE CONCENTRATES:

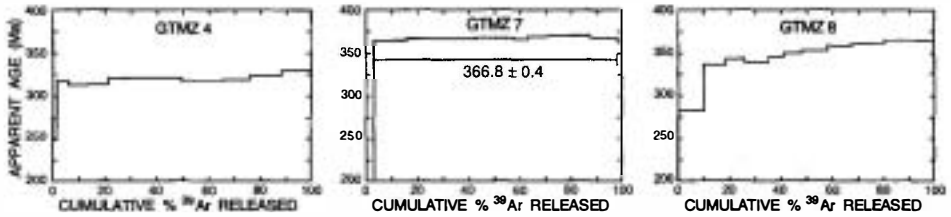

WHOLE-ROCK ANALYSES:

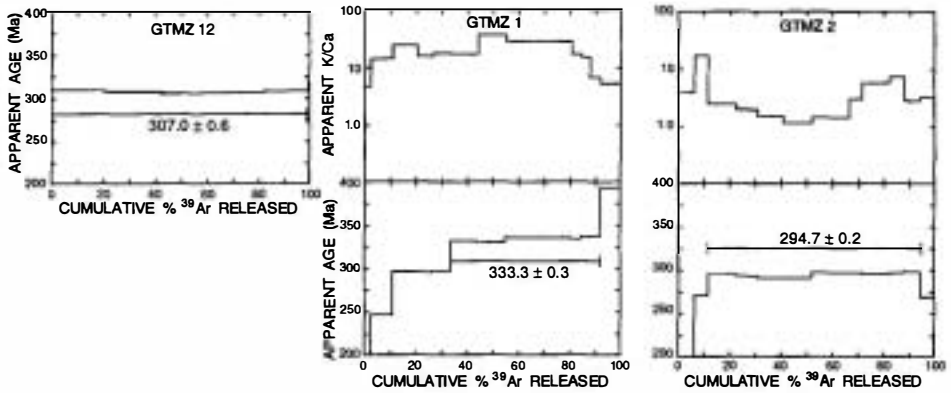

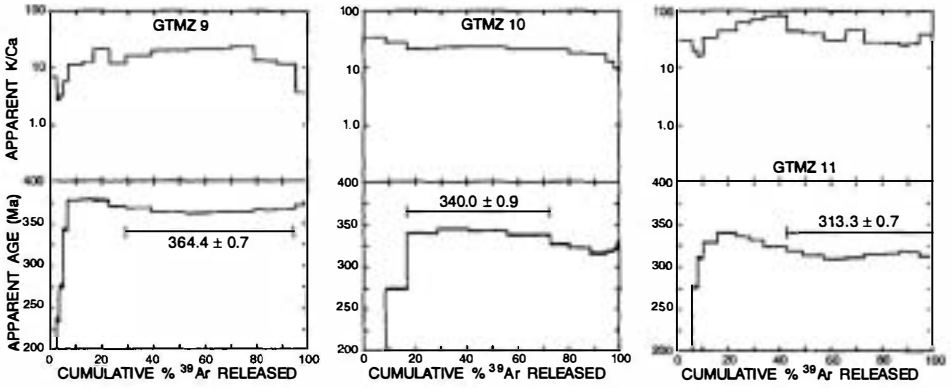

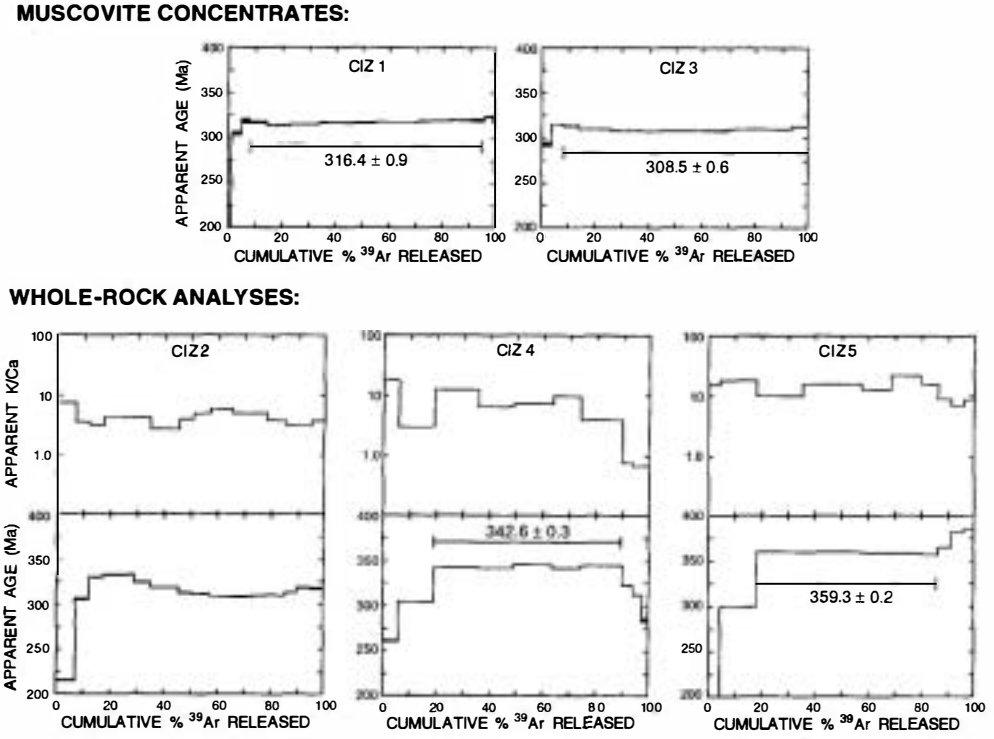

Fig. 7. $^{40}Ar/^{39}Ar$ apparent age of muscovite concentrates and whole-rock analyses from the Central Iberian Zone. Apparent K/Ca spectra are included for the whole-rock analyses. Data plotted as in Fig. 6.

does record partial rejuvenation, the 375 Ma defined by high-temperature increments may represent a minimum estimate for the cooling age. The cooling temperature for hornblende can be estimated at ca. 500°C, the transition from amphibolite to greenschist facies likely occurred during mylonitization, and the age may reflect relatively late stages of detachment evolution. Comparable $^{40}Ar/^{39}Ar$ mineral ages (372.8 ± 0.5 and 373.0 ± 0.5 Ma) were reported for mylonitic metagranite occupying a similar structural position in the Morais Complex (Dallmeyer et al., 1991).

5.1.2. GTMZ-5

Most intermediate- and high-temperature gas fractions evolved from the concentrate prepared from this sample display little intrasample variation in apparent K/Ca ratios, suggesting that experimental evolution of gas occurred from populations of compositionally uniform intracrystalline sites. These fractions record intrasample apparent ages corresponding to a plateau age of 432.1 ± 1.1 Ma. The plateau analytical data yield a well-defined $^{36}Ar/^{40}Ar$ vs. $^{39}Ar/^{40}Ar$ isotope correlation with an inverse ordinate intercept ($^{40}Ar/^{36}Ar$ ratio) that is not significantly different from the $^{40}Ar/^{36}Ar$ ratio in the present-day atmosphere. The intercept suggest no significant intracrystalline contamination with extraneous ('excess') argon components. Using the inverse ordinate intercept ($^{40}Ar/^{39}Ar$) in the age equation yields a plateau isotope correlation age of 425.2 ± 1.2 Ma. Because calculation of isotope correlation ages does not require assumption of a present-day $^{40}Ar/^{36}Ar$ ratio, this is more reliable than ages calculated directly from the analytical data.

The sample is a fine-grained, foliated, granonematoblastic amphibolite consisting of green amphibole (tschermakite to pargasitic hornblende), garnet, plagioclase (An_{35}), quartz and minor clinozoisite, scapolite, rutile, ilmenite and sphene. The amphibolite derives from the retrogression of a high-pressure mafic granulite with a mineral assemblage including

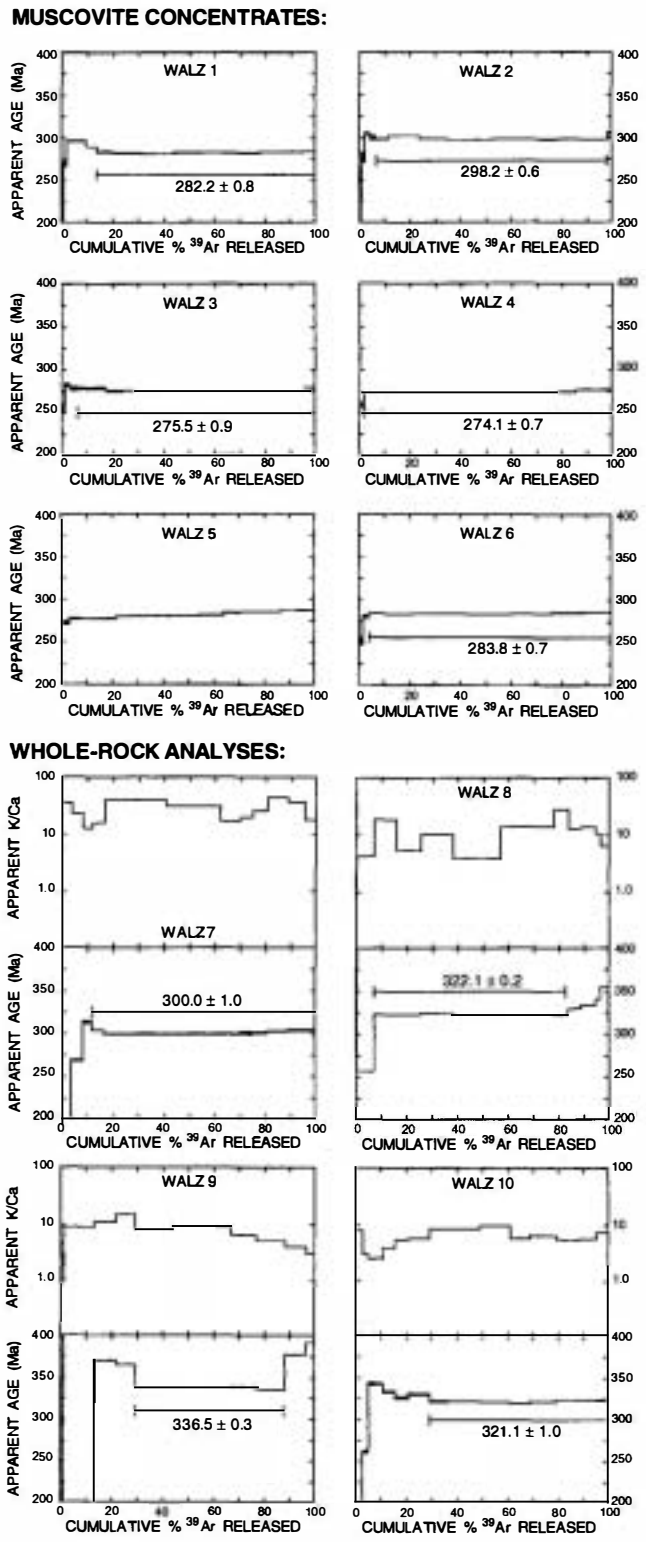

Fig. 8. $^{40}Ar/^{39}Ar$ apparent age of muscovite concentrates and whole-rock analyses from the West Asturian–Leonese Zone. Apparent K/Ca spectra are included for the whole-rock analyses. Data plotted as in Fig. 6.

clinopyroxene (now wholly replaced by hornblende), garnet, plagioclase, quartz and rutile. Most of the garnets exhibit a rounded shape, indicative of important ductile shearing during post-granulitic, mainly decompressive, stages.

Though the isotope correlation age of 425.2 ± 1.2 Ma is preferred for this sample, the geological significance is uncertain. It is apparent that the catazonal units underwent a subductive episode prior to, or during the very earliest phases of Variscan orogenesis. However, the precise age of this event has been controversial. Early Paleozoic isotopic ages ranging between ca. 480 and 490 Ma have been interpreted to date the HP–HT initial metamorphic event (Peucat et al., 1990). However, these have been considered to reflect protolith ages by Schäfer et al. (1993) and Santos Zalduegui et al. (1996a), who have dated the first metamorphic event in Cabo Ortegal at ca. 395 Ma and between 406 and 383 Ma, respectively. Furthermore, mineral ages of 380–390 Ma have been obtained from amphibolite-facies retrograded catazonal rocks at Cabo Ortegal (Van Calsteren et al., 1979; Peucat et al., 1990) and Bragança (Dallmeyer et al., 1991). If the isotope correlation age reflects last cooling of the hornblende grains, this would imply the possibility that the first tectonothermal events are older than suggested by Schäfer et al. (1993) and Santos Zalduegui et al. (1996a).

5.1.3. GTMZ-6

The intrasample apparent ages correspond to a plateau of 378.1 ± 0.4 Ma and the use of the inverse ordinate intercept ($^{40}Ar/^{39}Ar$) in the age equation yields a plateau isotope correlation age of 376.8±0.4 Ma. The rock is a medium-grained, well foliated, nematoblastic amphibolite with a mineral assemblage characteristic of the amphibolite facies: green amphibole (tschermakite to pargasitic hornblende), subidiomorphic garnet (up to 2 mm), plagioclase, quartz and minor epidote–clinozoisite, ilmenite and sphene. There is no evidence of older mineral assemblages, and the assemblage is considered to have crystallized at the metamorphic thermal peak. Considering that amphibole is not very different in composition from hornblende of sample GTMZ-3, though richer in Na(M4), a somewhat higher pressure of recrystallization under similar temperature is suggested. The plateau isotope correlation age of 376.8 ± 0.4 Ma is interpreted to relate to cooling following the amphibolite-facies metamorphism of upper ophiolitic units. This episode was followed by thrust-related shearing in greenschist-facies conditions and the age is therefore considered an estimate of the transition from one to the other tectonothermal events. It is similar to ages reported by Peucat et al. (1990) for equivalent rocks exposed in Cabo Ortegal.

5.2. Muscovite analyses

The twelve muscovite concentrates (Table 1) display variably discordant $^{40}Ar/^{39}Ar$ age spectra (Figs. 6–8). Apparent K/Ca ratios are very large, with considerable uncertainties and, consequently, are not shown with the age spectra. The K/Ca ratios display minor and non-systematic intrasample variations, suggesting that experimental evolution of gas occurred from compositionally uniform populations of intracrystalline sites. The muscovite concentrates generally record well-defined plateau ages, except those prepared from samples GTMZ-4, GTMZ-8 and WALZ-5. The plateau ages are interpreted to date the last cooling through temperatures required for intracrystalline retention of argon within constituent muscovite grains. Characteristics of the internally discordant spectra recorded by the muscovite concentrates prepared from samples GTMZ-4, GTMZ-8 and WALZ-5 are similar to those described from partially rejuvenated muscovite intracrystalline systems (e.g., Dallmeyer and Takasu, 1992). A similar interpretation may be appropriate in the present case; therefore no geologic significance is ascribed to the total-gas ages.

5.2.1. GTMZ-4

The rock is a high-pressure granulite-facies paragneiss retrogressed to the greenschist facies during mylonitization. The rock displays a schistosity with lepidoblastic muscovite and chlorite, which involve large (up to 3 mm) residual porphyroblastic garnets. These, together with some smaller and partially ilmenitized rutiles, are the main evidences of pre-mylonitic stages. Moreover, most of the plagioclase crystals (An_{15-20}) are intensively sericitized. Retrogressive muscovite in the schistosity is poor in paragonite and celadonite contents ($<Si_{3.1}$) and rich in Fe and Ti, suggesting relatively low pressure

of recrystallization. Though the release spectrum displays characteristics of partially rejuvenated intracrystalline systems, most temperature increments define apparent ages of ca. 325 Ma (Fig. 6), which can be considered a minimum estimate for the age of the last important resetting event. Interpretation of 300–330 Ma ages in this region is uncertain, because emplacement of syn-kinematic granitoids was roughly contemporaneous with D_3. Consequently, resetting can be explained either by recrystallization related with deformation, or by the thermal influx of nearby granite massifs. Furthermore, in many cases the latter might have influenced the former. In sample GTMZ-4, the ca. 325 Ma age is comparable to that of syn-kinematic granites emplaced in eastern Ordenes, which have yielded Rb–Sr whole-rock crystallization ages of 323 ± 11 Ma (Bellido et al., 1992).

5.2.2. GTMZ-7

The sample is a fine-grained granolepidoblastic schist constituted by garnet (smaller than 0.25 mm), muscovite (richer in paragonite content and poorer in Ti than that of sample GTMZ-4), chlorite, brown stilpnomelane, quartz and ilmenite. The rock displays a penetrative schistosity developed in the low-temperature part of the greenschist facies. Small garnets are previous to the schistosity, and appear partially replaced by micas. Some of them include an internal schistosity formed during an older and probably prograde event. This fact, together with the garnet growth preceding the development of the schistosity, suggests that the planar fabric has a decompressive character. A general refolding of the schistosity by open kink bands, represents the last event evident in the rock. In view of the nearly complete recrystallization which accompanied development of the schistosity, its low grade, the apparent absence of late thermal overprints and the small importance of the late folds, the obtained plateau age of 366.8 ± 0.4 Ma is interpreted to closely follow that of the greenschist-facies mylonitization event in the ophiolites of eastern Ordenes.

5.2.3. GTMZ-8

This is a sample from the lower ophiolitic units of the Ordenes Complex, and is a fine-grained lepidoblastic, muscovite-rich schist, consisting of green chloritoid (up to 0.5 mm), muscovite, chlorite, quartz and ilmenite. This low-temperature, chlorite zone schist, displays a penetrative schistosity defined by muscovite lepidoblasts, the chloritoid crystals being syn-kinematic to slightly previous to it. The dominant planar fabric is probably not the only schistosity developed in the rock, since a very thin previous one, almost erased, can still be identified. As in the previous case, muscovites are distinctly richer in paragonite content and poorer in Ti than those of sample GTMZ-4. The partial rejuvenation suggested by the release spectrum only permits a minimum estimate of the age of the last tectonothermal event. The apparent ages of the highest temperature increments, are ca. 363 Ma, and similar to the plateau age of sample GTMZ-7. They are interpreted in a similar way. These ages are comparable to a 370.2 ± 0.6 Ma date reported for phyllonite in the Morais ophiolites by Dallmeyer et al. (1991).

5.2.4. GTMZ-12

The rock is a medium-grained feldspathic quartzite constituted by quartz, sericitized plagioclase (An_8), biotite, muscovite and minor chlorite and opaque minerals. The rock exhibits an oriented granoblastic texture where mica lepidoblasts define the more evident planar fabric. Thermal effects associated to the adjacent granite do not have an obvious representation in the general texture, but some recrystallization restricted to the rim area of large quartz grains can be probably assigned to contact metamorphism. Muscovite and biotite are characterized by relatively high Ti contents. Temperature estimates for the equilibrium biotite–muscovite yield values of ca. 650°C for an assumed pressure of 5 kbar that are probably too high. The temperature of ca. 400°C at the same pressure, for the equilibrium muscovite–plagioclase is probably related to final retrogressive recrystallization of the rock. The obtained plateau age of 307.0 ± 0.6 Ma is interpreted as the cooling age following granite emplacement.

5.2.5. CIZ-1

This rock is a fine-grained, penetratively mylonitized, porphyritic rhyolite with preserved phenocrysts of quartz and, less abundant, plagioclase and K-feldspar, arranged in a highly sheared, low-temperature matrix with muscovite, brown stilp-

nomelane, microcrystalline quartz and pyrite. The mylonitic fabric is interpreted as S_2, on a regional basis, but no evidence of previous deformations has been preserved. The apparent ages obtained in the release spectrum probably do not reflect the mylonitization, because some of the microcrystalline quartzose mosaics appear recrystallized to secondary aggregates with larger grains showing polygonal textures. This recrystallization clearly post-dates the mylonitization and can be assigned to a slight thermal overprinting. Phengitic muscovite ($>Si_{3.3}$) is fairly rich in Mg and Fe and poor in paragonite component. Temperature estimates for the equilibrium muscovite–plagioclase are ca. 355 ± 10°C, for an assumed maximum pressure of 5 kbar. The plateau age of 316.4 ± 0.9 Ma (Fig. 7) is comparable to the crystallization ages reported for nearby granites and, in particular, to that of the Forgoselo massif, exposed to the west of As Pontes and ca. 6 km to the south of the sampling site (Fig. 4). An age of 314 ± 6 Ma has been reported for this massif by Capdevila and Vialette (1970) (corrected by Ries, 1979). However, as this is also the age of D_3 in the area according to these authors, interpretation has problems similar to those previously discussed for sample GTMZ-4.

5.2.6. CIZ-3

This medium-grained, two-mica monzogranite from the eastern limb of the Verín Synform shows a granular texture, with biotite, muscovite, quartz, plagioclase (An_{10-20}) and K-feldspar. Though mainly undeformed, some quartz grains exhibit undulose extinction or even appear recrystallized to secondary fine-grained mosaics. This subsolidus phenomenon, caused by minor deformation, can be related with local sericitization and saussuritization of the plagioclases, chloritization of biotites, as well as with the extended microclinization of the primary orthoclase grains. Biotite is moderately rich in Ti and Fe ($X_{Mg} = 0.38$), whereas primary muscovite is poor in celadonite and paragonite components, suggesting a relatively high temperature and low pressure of crystallization. The temperature for the equilibrium biotite–muscovite is 695 ± 35°C at an assumed pressure of 2 kbar. The plateau age of 308.5 ± 0.6 Ma is interpreted to date cooling subsequent to the granite emplacement. Note the similarity with the plateau age of sample GTMZ-12, interpreted also as a cooling age following granite emplacement, in the western limb of the Verín Synform.

5.2.7. WALZ-1 and WALZ-2

These samples were collected in an attempt to date the S_2 foliation in the Mondoñedo Nappe. Sample 1 is a highly sheared two-mica syenogranite with a well-developed S_2 foliation developed during the syn-kinematic emplacement of the massif. The high-temperature granolepidoblastic foliation is defined by the dimensional orientation of biotite, muscovite, quartz, K-feldspar and plagioclase (An_{10-15}). Muscovite is rich in Ti, Fe and Mg and poor in paragonite. Biotite is rich in Ti and Fe. The igneous compositions were variably changed through recrystallization since P–T estimates suggest disequilibrium among phases. Pressure estimates on the basis of the Si content of muscovite are around 4.5 ± 0.5 kbar for a temperature range of 500–700°C.

Sample 2 is a medium-grained porphyroblastic schist with a very penetrative medium-temperature schistosity. The mineral assemblage was probably developed during metamorphic peak conditions, and include muscovite, biotite, garnet, quartz, plagioclase (An_{15-20}) and ilmenite. The garnets show rotational textures, indicative of synschistose growth; this syntectonic character in relation to the single planar fabric can also be deduced for the rest of the fundamental minerals. Late retrogressive effects caused important chloritization of the garnets as well as sericitization of plagioclases. Garnets have grossular-rich cores (18 mol%) and preserve a growth zoning with X_{Mg} ratio increase and Mn contents decrease from core to rim. Muscovites are poor in Ti and celadonite component and rich in paragonite (18 mol%), whereas biotites are rich in Mg ($X_{Mg} = 0.53$). Peak-metamorphic conditions for the equilibrium of garnet rims with matrix plagioclase, biotite and muscovite were ca. 575±15°C and 6±0.3 kbar. Plateau ages of 282.2 ± 0.8 Ma and 298.2 ± 0.6 Ma are defined for samples 1 and 2, respectively (Fig. 8). These are considered too young to constrain the age of D_2 in the WALZ, because several whole-rock analyses described below, in samples collected eastward, give clearly older ages for the fold and thrust tectonics of the zone. For the first sample, collected near a post-kinematic granitoid (Fig. 4), the age is comparable to that obtained from the A

Tojiza pluton (WALZ-6), and to apparent ages for high-temperature increments of analysis of an adjacent country rock (WALZ-5). The second sample is comparable to WALZ-7 in the obtained age and in that both are from the Mondoñedo Nappe not so close to the post-kinematic massifs. This implies that S_2 was thermally overprinted during the intrusion of neighboring post-kinematic granitoids, and suggests that a different cause produced the 14–18 Ma older resetting in samples far from these massifs. Possibilities include a thermal event that preceded the emplacement of the post-kinematic granitoids or that the ca. 300 Ma ages are cooling ages related to unroofing of the Mondoñedo Nappe.

5.2.8. WALZ-3 and WALZ-4

Sample 3 is a fine-grained phyllonitic mica schist from the Mondoñedo Basal Thrust. It displays a very penetrative S_2 planar fabric with marked lenticular geometry, caused by anastomosed shear bands. This medium-temperature mica schist, consists of biotite, muscovite, quartz, plagioclase (An_{20}) and ilmenite, with chlorite, sericite and saussurite as located retrogressive products. Significative post-kinematic crystallization is deduced from the presence of biotites oblique to the mylonitic schistosity and of secondary granoblastic quartz-mosaics. Muscovite has a rather variable composition, though is generally rich in Fe and Mg. On the basis of maximum Si content of muscovite ($Si_{3.18}$), the phyllonitization took place at a pressure lower than 5 kbar. Temperature estimates for the equilibrium plagioclase–muscovite are ca. 500 ± 30°C. Sample 4 is a medium- to coarse-grained two-mica monzogranite with a granular undeformed texture, consisting of biotite, muscovite, quartz, plagioclase (An_{2-30}), K-feldspar and accessory minerals (including large tourmaline grains). As a significative process, the monzogranite appears affected by an important subsolidus, low-temperature hydration, with chloritization of biotites and saussuritization/sericitization of plagioclases. Probably also during this event, the primary orthoclase was transformed into microcline. Biotites are rich in Ti and Fe ($X_{Mg} = 0.27$), whereas muscovites are poor in celadonite and paragonite components, suggesting relatively high-temperature and low-pressure conditions of crystallization. Temperatures for the equilibrium biotite–muscovite are ca. 625 ± 20°C. The proximity of sampling sites for WALZ-3 and WALZ-4 (Figs. 4 and 5) and their similar plateau ages, 275.5 ± 0.9 Ma and 274.1 ± 0.7 Ma, respectively, support the conclusion that S_2 was thermally overprinted during intrusion of neighboring post-kinematic granitoids.

5.2.9. WALZ-5 and WALZ-6

Sample 5 is an originally foliated, granolepidoblastic mica schist, that was severely affected by thermal metamorphism. The older mineral assemblage, including muscovite, biotite, quartz, plagioclase and ilmenite, appears overprinted by large porphyroblasts of andalusite and smaller ones of cordierite. Some reduced and very restricted aggregates of fibrolitic sillimanite, generally developed after andalusite, were formed during the thermal peak. Later, an important low-temperature alteration, related with hydrothermal circulation, caused the almost complete replacement of andalusite by sericite, cordierite by pinite and biotite by chlorite. Biotite is moderately rich in Ti and Mg ($X_{Mg} = 0.39$). Very low Si contents ($<Si_{3.1}$) of muscovites, either aligned or transverse, suggest low-pressure conditions of recrystallization, which are consistent with the structural and petrographic features of the A Tojiza massif. Temperatures for the pair biotite–muscovite have been estimated at ca. 555 ± 10°C for an assumed maximum pressure of 2 kbar. Sample 6 is a coarse-grained, undeformed, two-mica syenogranite with inequigranular texture. The major mineralogy is formed by muscovite, biotite, quartz, K-feldspar and plagioclase (An_{2-35}). The presence of relatively abundant euhedral garnet crystals can be signaled. A last event of hydrothermal alteration caused chloritization of biotites and garnets and sericitization/saussuritization of plagioclases. Garnet is practically unzoned and extremely rich in Fe molecule (almandine >90 mol%), and the same is valid for biotite ($X_{Mg} = 0.07$). Crystallization took place under progressively lower pressure and temperature conditions down to a final stage at ca. 540±10°C and less than 2 kbar for the equilibrium of garnet rim–biotite–muscovite and plagioclase. Both samples were near each other and the 283.8 ± 0.7 Ma plateau age obtained from the A Tojiza pluton (WALZ-6), is similar to apparent ages around 280 Ma for high-temperature increments of the adjacent

country rock (WALZ-5), whose internally discordant $^{40}Ar/^{39}Ar$ spectrum suggests partial rejuvenation.

5.3. Whole-rock analyses

The twelve low-grade whole-rock samples (Table 1) display variably discordant apparent age spectra (Figs. 6–8). Variable and relatively young apparent ages are typically recorded in the small-volume increments evolved at low experimental temperatures, accompanied by relatively small and fluctuating apparent K/Ca ratios. Gas fractions liberated during intermediate-temperature portions of the analyses generally display very large and only slightly fluctuating apparent K/Ca ratios. Highest temperature increments typically display systematically decreasing apparent K/Ca ratios. Although the samples consist primarily of very fine-grained white mica, systematic intrasample variations in apparent K/Ca ratios suggest that several other phases likely contributed gas at various stages in the whole-rock analyses. Relative to white mica, these appear to have included: (1) a non-retentive phase present in variable modal abundance, with relatively low apparent K/Ca ratio; and (2) a more refractory phase with relatively low apparent K/Ca ratio, also present in minor modal abundance. Mineralogical characteristics and observed modal variations suggest that these phases may be chlorite and detrital plagioclase feldspar, respectively. Apparent ages recorded throughout intermediate- and initial high-temperature portions of the analyses are attributed to gas largely evolved from constituent, very fine-grained white mica. Except for slate sample CIZ-2, these gas fractions generally display little intrasample variation in apparent ages and define plateau ages.

Illite crystallinity values were determined for seven samples of low-grade slate and phyllonite (Table 1). Five samples reflect an upper anchizone grade and two a middle anchizone grade. These metamorphic conditions imply that Variscan metamorphic rejuvenation of constituent detrital micas was likely according to the work reported by Dallmeyer and Takasu (1992). Consequently, the $^{40}Ar/^{39}Ar$ plateau ages are considered geologically significant, and are interpreted to closely date the syn-kinematic growth of the fine-grained white-micas, or their thermal rejuvenation.

5.3.1. GTMZ-1 and GTMZ-2

The samples are phyllites displaying a single penetrative cleavage. In sample 1, it is defined by very fine muscovite lepidoblasts, with minor brown and green stilpnomelane and restricted chlorite. Besides quartz with undulose extinction, clastic albite grains are frequent. Sedimentary bedding is marked by layers with variable muscovite/stilpnomelane ratio. Sample 2 consists of muscovite, abundant chlorite and biotite. The latter appears in different generations displaying variable relationships with the cleavage, though late to post-schistose crystals are dominant and sometimes appear in restricted microgranoblastic quartz-rich domains where static recrystallization occurred. The $^{40}Ar/^{39}Ar$ plateau ages defined by these phyllites (Fig. 6) are Variscan, and do not record any pre-Variscan event. It is very doubtful if the age of 333.3 ± 0.3 Ma for GTMZ-1 may be interpreted to date cooling following the first deformation event in the uppermost units in the Ordenes Complex, because the Corredoiras Detachment, which post-dates the early compressive fabrics in the unit, is much older (at least 375 Ma, see discussion of sample GTMZ-3). Furthermore, the age corresponds to a partial plateau in a rising spectrum and probably represents a rejuvenation age related to D_3 folding or syn-D_3 granite emplacement. The single fabric of the rock may have recrystallized during the D_3 rotation and flattening of a former subhorizontal cleavage, as the sample was collected in the steep limb of a large D_3 fold. On the other hand, because the syn-kinematic granitoids are roughly contemporaneous to the D_3 event, we face again the problem, discussed for sample GTMZ-4, of distinguishing between the resetting due to deformation and that related to the influx of nearby granite massifs: the syn-kinematic Taboada massif, exposed east of the Ordenes Complex, has been dated by the Rb–Sr whole-rock method as 323 ± 11 Ma (Bellido et al., 1992). The 294.7 ± 0.2 Ma age of GTMZ-2 is similar to that of post-kinematic granitoids in this area. The massif of A Silva, exposed west of the sampling site, has yielded a Rb–Sr whole-rock crystallization age of 307 ± 20 Ma (Bellido et al., 1992).

5.3.2. GTMZ-9

The rock is a fine-grained phyllite displaying a very penetrative, mylonitic schistosity. In local-

ized domains, a previous cleavage can be identified. This chlorite zone metasediment contains a mineral assemblage constituted by muscovite, brown stilpnomelane, chlorite, quartz, albite and ilmenite. Temperature estimates for the equilibrium muscovite–plagioclase are under 400°C, even assuming pressures higher than 5 kbar for crystallization of phengitic muscovite. This sample, from the Cabo Ortegal Complex, is equivalent, petrographically and structurally, to samples GTMZ-7 and GTMZ-8 from the Ordenes Complex. Consequently, the plateau age of 364.4 ± 0.7 Ma is interpreted to closely date the greenschist-facies mylonitization in the lower ophiolitic units.

5.3.3. GTMZ-10

This sample is a very fine-grained phyllite with a penetrative cleavage as the only identifiable planar fabric. This low-temperature, chlorite-zone metapelite consists of muscovite, chlorite, brown stilpnomelane, quartz and opaque matter. Muscovite has a composition similar to that of muscovite from sample GTMZ-9, though with slightly lower contents in Fe and in paragonite molecule. Temperature estimates for the equilibrium muscovite–plagioclase are, as in the previous case, below 400°C. Illite crystallinity indicates an upper anchizone metamorphic grade. The $^{40}Ar/^{39}Ar$ spectrum is internally discordant, and the 340.0 ± 0.9 Ma age of the partial plateau must be considered in the light of the results from other samples also collected in the southern part of the study area. The much younger cooling age obtained for sample GTMZ-12 supports the petrographical conclusion that GTMZ-10 escaped the thermal influx of granitoids intruded to the west of the Verín Synform. On the other hand, the similarity of this age with that obtained from CIZ-4 and the possible continuity between the basal thrust of the schistose domain and the thrusts in the Alcañices Synform suggests that it may be related to tangential tectonics (D_1 and, more probably, D_2) recorded in the schistose domain.

5.3.4. GTMZ-11

This sample is a fine-grained phyllonitic metapelite. The chlorite-zone mylonite consists of muscovite, chlorite, brown stilpnomelane, quartz, albite and very abundant opaque matter, mainly graphitic. The mylonitic schistosity has not allowed the preservation of any previous planar fabric, whose presence must be nevertheless considered in the basis of regional data. It shows a characteristic lenticular geometry, due to the anastomosed shearing of quartz-rich bands, probably generated in the early stages of the mylonitic event. Muscovite has lower contents in celadonite ($<Si_{3.1}$) than muscovites from samples GTMZ-9 and GTMZ-10, which suggests recrystallization under slightly lower pressure conditions. Illite crystallinity indicates an upper anchizone metamorphic grade close to the greenschist facies. The sample was collected to date the basal thrust of the schistose domain. The 313.3 ± 0.7 Ma age corresponds to a partial plateau in a disturbed spectrum and probably represents a rejuvenation age. It may relate to the thermal influence of syn-kinematic granites as suggested by the 307.0 ± 0.6 Ma age obtained for sample GTMZ-12.

5.3.5. CIZ-2

The rock is a slate consisting of muscovite (rich in paragonite, up to 18 mol%, and poor in Si, Ti, Fe and Mg), chlorite, quartz, albite (An_{8-10}), pyrite and opaque matter including abundant graphite. It displays a penetrative S_1 cleavage, later affected by a slight crenulation without significative recrystallization. Illite crystallinity indicates an upper anchizone metamorphic grade. The $^{40}Ar/^{39}Ar$ analysis displays an internally discordant apparent age spectrum with uncertain significance (Fig. 7), but probably related to rejuvenation. This is not surprising in view of the proximity of this sample to GTMZ-11 (Figs. 4 and 5), in which the rejuvenation seems related to the thermal influence of syn-kinematic granites. Apparent ages of approximately 309 Ma for the intermediate- and high-temperature increments are comparable to the cooling ages of 308.5 ± 0.6 Ma in a granite exposed to the east of the Verín Synform (CIZ-3), and 307.0 ± 0.6 Ma of sample GTMZ-12, probably with a similar significance but in the western limb of the synform.

5.3.6. CIZ-4 and CIZ-5

These low-grade metapelites were collected far from any granitic massif, and appear to have escaped the influx of thermal rejuvenation and have provided two interesting key ages. Sample 4 is a

very fine-grained phyllite displaying a well developed S_2 crenulation cleavage. The rock contains a chlorite-zone mineral assemblage consisting of muscovite, chlorite and quartz, with less abundant brown stilpnomelane and opaque matter. Phengitic muscovites are distinctly richer in celadonite ($Si_{3.3}$) and poorer in paragonite than those from sample CIZ-2, which suggests a somewhat higher pressure of metamorphism. There are no differences in chemical composition between the muscovites of the two planar fabrics. Sample 5 is a slate displaying a single and penetrative S_1 cleavage. The mineral assemblage, typical of the chlorite zone, is syn-kinematic and constituted by muscovite, chlorite, quartz, abundant chloritoid and opaque matter including graphite. The chemical composition of muscovite is distinctly poorer in celadonite and richer in paragonite components than in sample CIZ-2. Illite crystallinity indicates a middle anchizone metamorphic grade for both samples. As stated previously, Variscan metamorphic rejuvenation of constituent detrital micas can be assumed for these metamorphic conditions (Dallmeyer and Takasu, 1992). Consequently, the $^{40}Ar/^{39}Ar$ plateau ages of 342.6 ± 0.3 Ma for sample 4 and 359.3 ± 0.2 Ma for sample 5 are considered geologically significant, and are interpreted to closely date the syn-kinematic growth of the fine-grained white-micas or the thermal rejuvenation of pre-existing detrital micas, during cleavage formation. CIZ-4 is interpreted to closely date D_2 thrusting along the eastern limb of the Alcañices Synform, whereas CIZ-5 constrains the age of the S_1 cleavage developed within the Ollo de Sapo Anticline.

5.3.7. WALZ-7

This rock is a fine-grained metagraywacke from the chlorite zone, displaying a single penetrative S_1 cleavage. Muscovite, biotite, brown stilpnomelane, quartz, albitic plagioclase and opaque minerals define the mineral assemblage, apparently developed during metamorphic peak conditions. Muscovite has variable contents in celadonite ($Si_{3.04-3.21}$) and paragonite components (3–10 mol%). Temperature estimates for the equilibrium plagioclase–muscovite are around 400 ± 20°C, for an assumed maximum pressure of 5 kbar. The plateau age of 300.0 ± 1.0 Ma (Fig. 8) appears too young to constrain the age of D_1 in the WALZ, for the reasons outlined in the discussion of the muscovite analysis of sample WALZ-2. The comparable ages of WALZ-2 and WALZ-7 suggest similar interpretations.

5.3.8. WALZ-8 and WALZ-9

These low-grade metapelites display a penetrative S_1 cleavage and were aimed to date the D_1 event. Sample 8 is a slate, with S_1 slightly folded by spaced open kink bands, and with a syn-kinematic mineral assemblage constituted by chlorite, muscovite, quartz, albite and opaque matter with abundant graphite. Muscovite is poor in celadonite and moderately rich in the paragonite component (10 mol%), suggesting low-grade conditions for the metamorphism. Temperature estimates for the equilibrium plagioclase–muscovite are around 340 ± 10°C, for an assumed maximum pressure of 5 kbar. Sample 9 is a phyllite from the chlorite zone, with a syn-kinematic mineral assemblage, developed during metamorphic peak conditions, consisting of chlorite, muscovite, quartz, albite and ilmenite. Muscovite is poor in celadonite and relatively rich in paragonite components. This suggests low-grade conditions of metamorphism. Temperature estimates for the equilibrium plagioclase–muscovite are around 300 ± 10°C, for an assumed maximum pressure of 5 kbar. Illite crystallinity indicates an upper anchizone metamorphic grade for both samples. Again, this implies that Variscan metamorphic rejuvenation of constituent detrital micas was likely, and the $^{40}Ar/^{39}Ar$ plateau ages are considered geologically significant (Dallmeyer and Takasu, 1992). The plateau age of 336.5 ± 0.3 Ma obtained from WALZ-9 is interpreted to closely date syn-kinematic growth of the fine-grained white-micas or the thermal rejuvenation of pre-existing detrital micas, during S_1 development. The release spectrum of WALZ-8 depicts an excellent plateau, but its age, 322.1 ± 0.2 Ma, appears comparatively young relative to WALZ-9. The rising aspect of the spectrum suggest some rejuvenation. As the sample was collected within a zone affected by S_3 crenulation cleavage, the age may correspond to a resetting due to D_3 deformation.

5.3.9. WALZ-10

This rock is a phyllonite consisting of a groundmass of fine-grained, aligned muscovite (S_2) containing discontinuous bands rich in fine-grained

quartz and chlorite. Poorly oriented muscovite crystals within quartz-rich bands may correspond to a previous fabric (S_1). Albitic plagioclase, tourmaline, iron sulfides and rutile occur in lesser amounts. Muscovite is moderately rich in celadonite ($Si_{3.2}$) and poor in paragonite contents (5 mol%), which suggests an intermediate-pressure regime of metamorphism. Temperature estimates for the equilibrium plagioclase–muscovite are around 300 ± 10°C, for an assumed maximum pressure of 5 kbar. This permits consideration of the 321.1 ± 1.0 Ma plateau age as geologically significant. The age is interpreted as approximately dating the Trones Thrust and, consequently, it is considered representative of D_2 in the boundary between the WALZ and the CZ.

6. Geological significance

The $^{40}Ar/^{39}Ar$ results suggest that an extensive regional thermal influence developed during emplacement of the numerous Variscan granites exposed in the study area. At least seven of the metamorphic rocks record the effects of partial or complete rejuvenation during intrusion of neighboring granite massifs and for three more samples, this influence is also probable, though the rejuvenation may have been also caused by syn-D_3 recrystallization.

Where fabric ages have been constrained by the $^{40}Ar/^{39}Ar$ results, the new data confirm that the Iberian Variscan orogen is internally complex and has been affected by deformational processes manifested by contrasting tectonometamorphic events in different places. But also, and together with the previously published data, they permit establishment of estimates of the diachronism and the propagation rates during the orogenic process. The diachronous character of the first tectonothermal episodes can be appreciated in Fig. 9.

A group of samples from the tectonostratigraphically highest catazonal and ophiolitic units in the Ordenes and Cabo Ortegal complexes gives ages of ca. 380–365 Ma (Middle–Late Devonian). The oldest age (377 Ma), corresponds to the prograde amphibolite-facies event in the upper ophiolites of the Ordenes Complex. This is comparable to 390–380 Ma ages previously reported for ophiolitic units in Cabo Ortegal and the Portuguese complexes, and to the ages of amphibolite-facies retrograde recrystallization in catazonal units of Cabo Ortegal and Morais (Peucat et al., 1990; Dallmeyer and Gil Ibarguchi, 1990; Dallmeyer et al., 1991). These and a similar approximate age for the Corredoiras Detachment are also comparable to an age of 374 Ma previously reported for growth of post-eclogitic white mica in basal units of the Malpica–Tui Complex (Van Calsteren et al., 1979).

The new $^{40}Ar/^{39}Ar$ data suggest that prograde metamorphism affected the ophiolitic units while structurally overlying catazonal and uppermost units were decompressed and basal units subducted (Martínez Catalán et al., 1996). Prograde evolution of the catazonal units predated this stage. The granulitic/eclogitic metamorphism recorded must have been 'early' Variscan because of the single-loop geometry of associated *P–T–t* paths (Arenas, 1991). However, its precise age and tectonic significance in the overall Variscan orogenic cycle is uncertain. The significance of the 425 Ma $^{40}Ar/^{39}Ar$ hornblende age reported here for retrograded mafic granulite in Ordenes, is uncertain in view of the fact that the HP–HT metamorphism in similar rocks of the Cabo Ortegal Complex has been dated at ca. 395 Ma (Schäfer et al., 1993; Santos Zalduegui et al., 1996a).

The youngest $^{40}Ar/^{39}Ar$ ages herein reported for crystalline complexes are recorded in greenschist-facies mylonitic ophiolites (ca. 365 Ma). These are in same the range (or slightly older) as the oldest ages obtained for D_1 in the relative autochthon (359 Ma in the normal limb of the Ollo de Sapo Anticline), and suggest that deformation in the CIZ generally post-dated all regional-scale deformational fabrics developed in the allochthonous complexes (which in the Upper Devonian were palinspastically located to the west of their present position). The 359 Ma age helps constrain the age of the San Vitero Fm. (Alcañices Synform) because it was deformed by D_1 (Antona and Martínez Catalán, 1990). Therefore this synorogenic flysch must be of Devonian age.

Final emplacement of allochthonous complexes probably occurred shortly before that of the schistose domain, which appears to have occurred in the Lower Carboniferous (Visean–Tournaisian) in Verín and Alcañices. Deformation appears to have propagated eastward, reaching the eastern limit of the WALZ in the middle Visean (336 Ma: age of S_1 in Cudillero, see Fig. 4).

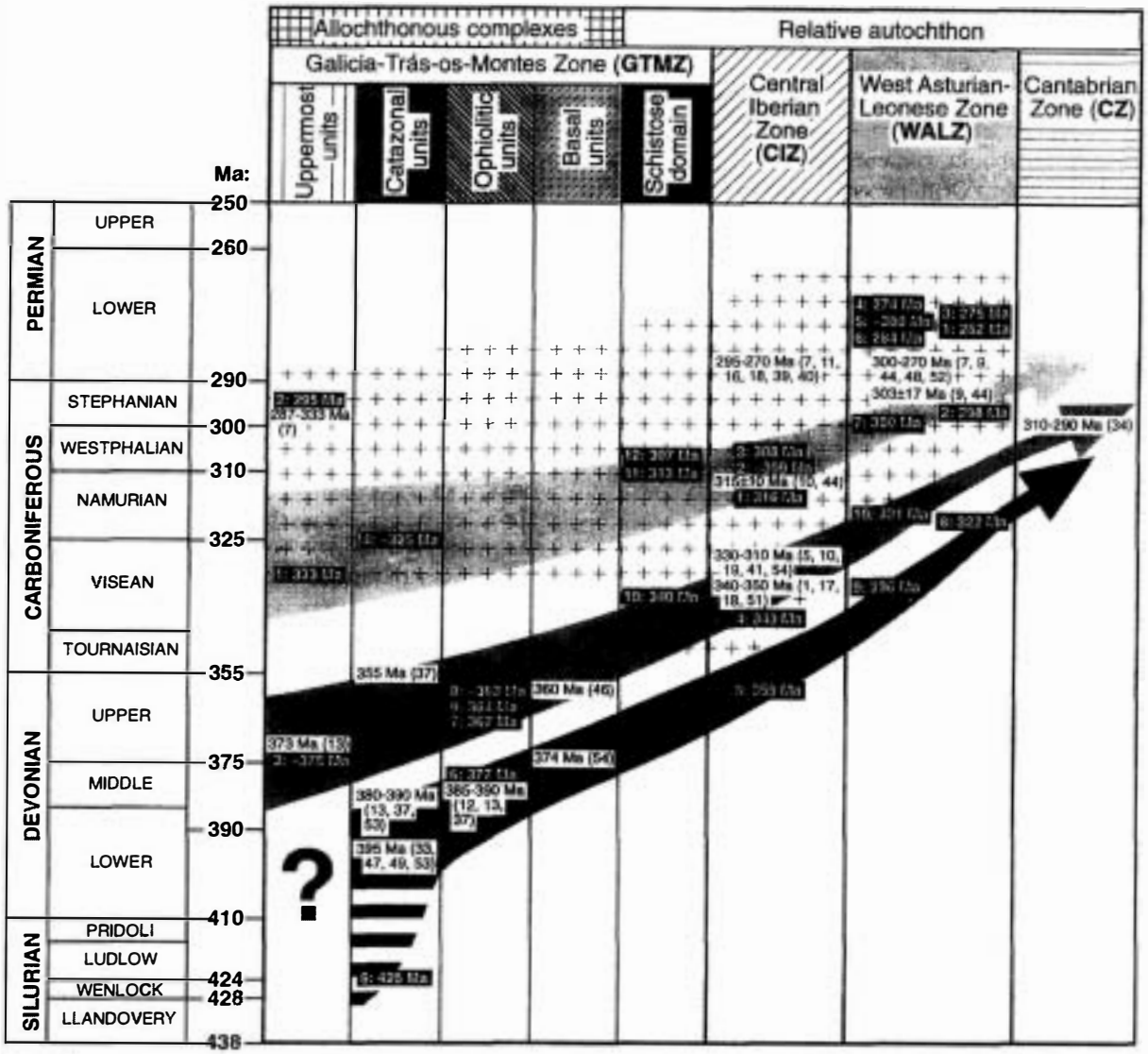

Obtained age (this study). The sample number is indicated for every zone.

374 Ma (54) Published age with reference (see list in Fig. 3).

First metamorphism and deformation episodes: HP events in catazonal and basal units, amphibolite facies event in ophiolitic units, D1 in the schistose domain, CIZ and WALZ. Beginning of thrust tectonics in the CZ.

Second metamorphism and deformation episodes, mainly thrust faults and early extensional detachments: amphibolite facies mylonitization in catazonal units, imbrication of the ophiolites and thrusting of the basal units. D2 in the schistose domain, CIZ and WALZ. Continuation of thrust tectonics in the CZ.

Late deformations: D3 Steep folds and transcurrent shear zones. Late extensional detachments.

Granite intrusions and accompanying thermal effects.

The $^{40}Ar/^{39}Ar$ data confirm the overall deformational sequence proposed by Pérez-Estaún et al. (1991) for the footwall to the suture: deformation propagating eastward with structures of different phases originated at the same time in different places. For instance, D_1 recumbent folds and S_1 cleavage appear to have formed in the WALZ at approximately the same time (336 Ma at its easternmost parts) that the schistose domain (with the allochthonous complexes already structurally emplaced on top) was translated over the CIZ along a D_2 thrust fault (340–343 Ma). D_2 thrusting affected the WALZ–CZ boundary in the lower Namurian (321 Ma), and then propagated eastward as the first deformational event.

7. Concluding remarks

The various Variscan deformational phases are considered to represent local responses to regional shortening. The local manifestations of the various deformational events varied with local *P–T* conditions and previous strain history. They should not be considered as contemporaneous, distinct orogen-wide events. For instance, in preserved parts of internal zones structurally underlying the allochthonous complexes, a regional first episode of ductile deformation led to formation of recumbent folds (D_1) and S_1 cleavage. This was followed by localization of tangential D_2 deformation in ductile shear zones and thrusts. This entire deformational sequence migrated eastward with time, with local complications resulting from development of gravitationally induced extensional detachments (Escuder Viruete et al., 1994; Díez Balda et al., 1995) and generation of late steep folds (D_3).

In the context of the orogenic wedge model of Platt (1986), Variscan deformation propagated eastward as new material was added to its front; however, the entire wedge remained active, with different structures locally produced at different times. An estimate of the overall propagation rate can be obtained by comparing isotopic ages defined for D_1 in the normal limb of the Ollo de Sapo Anticline (359 Ma) and in Cudillero (336 Ma). This corresponds to 23 Ma for locations presently separated by 125 km (Fig. 4). A similar time span is obtained when comparing ages of D_2 mylonites in Alcañices (343 Ma) and the Trones Thrust (321 Ma). These values imply that the foreland crust being added every million of years along the front of the Variscan tectonic wedge, became 5 km of deformed crust, after having undergone several deformative events. Considering hypothetical values for orogenic shortening of 50 and 75%, the estimated rate of 5 km/m.y. of formation of orogenic wedge equate to 10 and 20 km of foreland crust incorporated into the wedge every million year. This would have reflected an average convergence rate of 1–2 cm/year.

Development of late structures was also related to dynamics within the wedge, but their temporal development appears to have been less constrained by migration rates, as reflected by the weak inclination of the lighter arrow of Fig. 9. For instance, D_3 folds developed as a consequence of thrust activity below (either as fault-bend folds or caused by antiformal stacks) or in relationship to vertical, transcurrent ductile shear zones. The 322 Ma age obtained in Luarca, probably a D_3 age, is similar to that of the Trones Thrust (321 Ma); therefore both could be genetically related. However, an age of 315 ± 10 Ma for D_3 in the more internal Ollo de Sapo, is apparently younger and perhaps related to the Palas de Rei transcurrent shear zone (Iglesias Ponce de León and Choukroune, 1980).

The ca. 300 Ma ages obtained from samples of the Mondoñedo Nappe may be interpreted as cooling ages related to unroofing of the nappe. These ages have been obtained in rocks around the Xistral Tectonic Window (Figs. 2 and 5), which are exposed because of the development of a late, open antiform. This structure was considered by Pérez-Estaún et

Fig. 9. Plot of the new $^{40}Ar/^{39}Ar$ and previously available ages in a space–time diagram, showing the diachronism of the main tectonothermal events across the NW Iberian Massif. The time scale is uniform and based on the time-scale calibration of Cowie and Basset (1989). The zones and units (columns) are ordered in their original relative positions, loosely indicating the space horizontal coordinate transverse to the orogenic belt. The more internal zones and units, supposed to have occupied the westernmost positions (in present coordinates), are depicted to the left, and the more external, occupying the easternmost position, to the right.

al. (1991) to relate to formation of an antiformal stack during underthrusting of the basement of the Cantabrian Zone to the west while the sediments of this zone were detached and stacked forming the thin-skinned external thrust belt. This hypothesis seems confirmed by the seismic profile ESCI-N3.3 (Martínez Catalán et al., 1995) and has been included in Fig. 5, Section II. It would imply an age for the development of the antiform roughly contemporaneous to that of the thrusting in the western part of the CZ, which is early Westphalian (Pérez-Estaún et al., 1988). Consequently, the ages under discussion are probably related to unroofing of the Mondoñedo Nappe, induced by development of an underlying antiformal stack, and linked to advanced stages of the dynamics of the orogenic wedge.

Acknowledgements

This study was financed by grant GEO91-1470-E from the Spanish CICYT, and the research projects PB91-0192-C02, PB95-1035 and PB94-1396-C02 from the Spanish DGICYT and EB033/93 of the UPV-EHU. P. Gervas participated in the first sampling campaign and provided samples from the ophiolitic units of Ordenes. M. Hacar and L.M. Martín Parra provided sample locations in the Alcañices Synform. J.R. Wijbrans and an anonymous referee made constructive reviews of an initial version of the paper. Their comments and suggestions are greatly appreciated and have contributed to the improvement of the final version.

References

Abranches, M.C.B., Canilho, M.H. and Canêlhas, M.G.S., 1979. Idade absoluta pelo método do Rb/Sr dos granitos do Porto e de Portalegre (Nota preliminar). Bol. Soc. Geol. Portugal, 21: 239–248.

Allegret, A. and Iglesias Ponce de León, M., 1987. U–Pb dating of Sisargas orthogneisses (Galicia, NW-Spain): new evidence of a Precambrian basement in the northwestern part of the Iberian Peninsula. Neues Jahrb. Mineral. Monatsh., 8: 355–368.

Aller, J., Bastida, F., Brime, C. and Pérez-Estaún, A., 1987. Cleavage and its relation with metamorphic grade in the Cantabrian Zone (Hercynian of North-West Spain). Sci. Geol. Bull., 40: 1–18.

Antona, J.F. and Martínez Catalán, J.R., 1990. Interpretación de la Formación San Vitero en relación con la Orogenia Hercínica. Cuad. Lab. Xeol. Laxe, 15: 257–269.

Arenas, R., 1991. Opposite *P*, *T*, *t* paths of Hercynian metamorphism between the upper units of the Cabo Ortegal Complex and their substratum (northwest of the Iberian Massif). Tectonophysics, 191: 347–364.

Arenas, R., Gil Ibarguchi, J.I., González Lodeiro, F., Klein, E., Martínez Catalán, J.R., Ortega Girones, E. Pablo Maciá, J.G. de and Peinado, M., 1986. Tectonostratigraphic units in the complexes with mafic and related rocks of the NW of the Iberian Massif. Hercynica, 2: 87–110.

Arenas, R., Rubio Pascual, F.J., Díaz García, F. and Martínez Catalán, J.R., 1995. High-pressure micro-inclusions and development of an inverted metamorphic gradient in the Santiago Schists (Ordenes Complex, NW Iberian Massif, Spain): evidence of subduction and syn-collisional decompression. J. Metamorphol. Geol., 13: 141–164.

Autran, A. and Cogné, J., 1980. La zone interne de l'Orogenèse Varisque dans l'Ouest de la France et sa place dans le développement de la Chaîne Hercynienne. Coll. C6. 26 Congr. Géol. Int.: Géologie de l'Europe. Mém. B.R.G.M., 108: 90–111.

Barr, S.M. and Areias, L., 1980. Petrology and geochemistry of granitic intrusions in the Viana do Castelo area. Northern Portugal. Geol. Mijnbouw, 59: 273–281.

Bastida, F., Martínez Catalán, J.R. and Pulgar, J.A., 1986. Structural, metamorphic and magmatic history of the Mondoñedo nappe (Hercynian belt, NW Spain). J. Struct. Geol., 8: 415–430.

Bellido, F., Brandle, J.L., Lasala, M. and Reyes, J., 1992. Consideraciones petrológicas y cronológicas sbre las rocas graníticas hercínicas de Galicia. Cuad. Lab. Xeol. Laxe, 17: 241–261.

Bellido Mulas, F., González Lodeiro, F., Klein, E., Martínez Catalán, J.R. and de Pablo-Maciá, J.G., 1987. Las rocas graníticas hercínicas del Norte de Galicia y occidente de Asturias. Mem. Inst. Geol. Min. Esp., 101, 157 pp.

Bernard-Griffiths, J., Peucat, J.J., Cornichet, J., Iglesias Ponce de León, M. and Gil Ibarguchi, J.I., 1985. U–Pb, Nd isotope and REE geochemistry in eclogites from the Cabo Ortegal Complex, Galicia, Spain: an example of REE immobility conserving MORB-like patterns during high-grade metamorphism. Chem. Geol., 52: 217–225.

Blaise, J. and Bouyx, E., 1980. Les séries cambro-ordoviciennes à Cruziana et le problème de l'extension septentrionale des plate-formes 'perigondwaniennes' durant le Paléozoïque inférieur. C.R. Acad. Sci. Paris, 291: 793–796.

Brown, E.H., 1977. The crossite content of Ca-amphibole as a guide to pressure of metamorphism. J. Petrol., 18: 53–72.

Capdevila, R. and Vialette, Y., 1965. Premières mesures d'âge absolu effectuées par la méthode au strontium sur des granites et micaschistes de la province de Lugo (Nord-Ouest de l'Espagne). C.R. Acad. Sci. Paris, 260: 5081–5083.

Capdevila, R. and Vialette, Y., 1970. Estimation radiométrique de l'âge de la deuxième phase tectonique hercynienne en Galice Moyenne (Nord-Ouest de l'Espagne). C.R. Acad. Sci. Paris, 270: 2527–2530.

Cocherie, A., 1978. Géochimie des terres rares dans les granitoïds. Ph.D. Thesis. Univ. Rennes, 207 pp.

Corretgé, L.G., Suárez, O. and Galán, G., 1990. West Asturian–

Leonese Zone. Igneous Rocks. In: R.D. Dallmeyer and E. Martínez García (Editors), Pre-Mesozoic Geology of Iberia. Springer-Verlag, Berlin, pp. 115–128.

Cowie, J.W. and Basset, M.G., 1989. I.U.G.S. 1989 Global Stratigraphic Chart. Episodes, 12(2), Supplement.

Dallmeyer, R.D. and Gil Ibarguchi, J.I., 1990. Age of amphibolitic metamorphism in the ophiolitic unit of the Morais allochthon (Portugal): implications for early Hercynian orogenesis in the Iberian Massif. J. Geol. Soc. London, 147: 873–878.

Dallmeyer, R.D. and Takasu, A., 1992. $^{40}Ar/^{39}Ar$ ages of detrital muscovite and whole-rock slate/phyllite, Narragansett Basin, RI-MA, USA: implications for rejuvenation during very low-grade metamorphism. Contrib. Mineral. Petrol., 110: 515–527.

Dallmeyer, R.D. and Tucker, R.D., 1993. U–Pb zircon age for the Lagoa augen gneiss, Morais Complex, Portugal: tectonic implications. J. Geol. Soc. London, 150: 405–410.

Dallmeyer, R.D., Ribeiro, A. and Marques, F., 1991. Polyphase Variscan emplacement of exotic terranes (Morais and Bragança Massifs) onto Iberian successions: Evidence from $^{40}Ar/^{39}Ar$ mineral ages. Lithos, 27: 133–144.

De Bruiyn, H., Van Der Westhuizen, W.A. and Schoch, A.E., 1983. The estimation of FeO, F and H_2O^+ by regression in microprobe analyses of natural biotite. J. Trace Microprobe Technol., 1: 399–413.

Díaz García, F., 1990. La geología del sector occidental del Complejo de Ordenes (Cordillera Hercínica, NW de España). Nova Terra, 3, 230 pp.

Díez Balda, M.A., Vegas, R. and González Lodeiro, F., 1990. Central-Iberian Zone. Autochthonous Sequences. Structure. In: R.D. Dallmeyer and E. Martínez García (Editors), Pre-Mesozoic Geology of Iberia. Springer-Verlag, Berlin, pp. 172–188.

Díez Balda, M.A., Martínez Catalán, J.R and Ayarza, P., 1995. Syn-collisional extensional collapse parallel to the orogenic trend in a domain of steep tectonics: the Salamanca detachment zone (Central Iberian Zone, Spain). J. Struct. Geol., 17: 163–182.

Droop, G.T.R., 1987. A general equation for estimating Fe^{3+} concentrations in ferromagnesian silicates and oxides from microprobe analyses, using stoichiometric criteria. Min. Mag., 51: 431–435.

Escuder Viruete, J., Arenas, R. and Martínez Catalán, J.R., 1994. Tectonothermal evolution associated with Variscan crustal extension in the Tormes Gneiss Dome (NW Salamanca, Iberian Massif, Spain). Tectonophysics, 238: 117–138.

Farias, P., 1990. La geología de la región del Sinforme de Verín (Cordillera Herciniana, NW de España). Nova Terra, 2, 201 pp.

Farias, P., Gallastegui, G., González-Lodeiro, F., Marquínez, J., Martín-Parra, L.M., Martínez Catalán, J.R., de Pablo-Maciá, J.G. and Rodríguez-Fernández, L.R., 1987. Aportaciones al conocimiento de la litoestratigrafía y estructura de Galicia Central. Mem. Fac. Ciênc., Univ. Porto, 1: 411–431.

Fombella Blanco, M.A., 1984. Age palynologique du blastomilonitic Grabben, Zone Occidentale de la Galice. Rev. Micropaléontol., 27: 113–117.

Fourcade, S., Peucat, J.J., Martineau, F., Cuesta, A., Corretgé, L.G. and Gil Ibarguchi, J.I., 1989. Análisis de isótopos de oxígeno y edad Rb–Sr del plutón zonado de Caldas de Reyes (Galicia, España). Geogaceta, 6: 7–9.

Gallastegui, G., 1993. Petrología del macizo granodiorítico de Bayo-Vigo (Provincia de Pontevedra, España). Ph.D. Thesis, Univ. Oviedo, 363 pp.

García Garzón, J., 1987. Datación por el método Rb–Sr de dos muestras de granito de Galicia: granito tipo Padrón y granito tipo Porriño. Bol. Geol. Min., 98: 695–698.

García Garzón, J. and Locutura, J., 1981. Datación por el método Rb–Sr de los granitos de Lumbrales-Sobradillo y Villar de Ciervo-Puerto Seguro. Bol. Geol. Min. Esp., 92: 68–72.

García Garzón, J., de Pablo-Maciá, J.G. and Llamas Borrajo, J.F., 1981. Edades absolutas obtenidas mediante el método Rb/Sr en dos cuerpos de ortoneises en Galicia Occidental. Bol. Geol. Min. Esp., 92: 463–466.

Gebauer, D., 1993. Intra-grain zircon dating within the Iberian Massif: Ollo de Sapo augengneisses, bimodal gneisses from the Massif de Guilleries (Girona), graywacke of the Tentudía Group (Serie Negra, SW Spain) and the HP/HT-rock association at Cabo Ortegal (Galicia). Com. XII Reuniao Geol. Oeste Peninsular, Univ. Evora, 2: 41–46.

Gil Ibarguchi, J.I., 1995. Petrology of jadeite–metagranite and associated orthogneiss from the Malpica–Tuy allochthon (Northwest Spain). Eur. J. Mineral., 7: 403–415.

Gil Ibarguchi, J.I. and Arenas, R., 1990. Metamorphic evolution of the allochthonous complexes from the northwest of the Iberian Peninsula. In: R.D. Dallmeyer and E. Martínez García (Editors), Pre-Mesozoic Geology of Iberia. Springer-Verlag, Berlin, pp. 237–246.

Gil Ibarguchi, J.I. and Dallmeyer, R.D., 1991. Hercynian blueschist metamorphism in North Portugal: tectonothermal implications. J. Metamorphol. Geol., 9: 539–549.

Gil Ibarguchi, I. and Ortega Gironés, E., 1985. Petrology, structure and geotectonic implications of glaucophane-bearing eclogites and related rocks from the Malpica–Tuy (MT) Unit, Galicia, Northwest Spain. Chem. Geol., 50: 145–162.

Green, N.L. and Usdansky, S.I., 1986. Toward a practical plagioclase–muscovite thermometer. Am. Mineral., 71: 1109–1117.

Gutiérrez-Alonso, G., 1996. Strain partitioning in the footwall of the Somiedo Nappe: structural evolution of the Narcea Tectonic Window, NW Spain. J. Struct. Geol., 18: 1217–1229.

Gutiérrez-Alonso, G. and Nieto, F., 1996. White-mica 'crystallinity', finite strain and cleavage development across a large Variscan structure, NW Spain. J. Geol. Soc., London, 153: 287–299.

Hoisch, T.D., 1989. A muscovite–biotite geothermometer. Am. Mineral., 74: 565–572.

Hoisch, T.D., 1990. Empirical calibration of six geobarometers for the mineral assemblage quartz + muscovite + biotite + plagioclase + garnet. Contrib. Mineral. Petrol., 104: 225–234.

Holland, T.J.B. and Blundy, J.D., 1994. Non-ideal interactions in calcic amphiboles and their bearing on amphibole–plagioclase thermometry. Contrib. Mineral. Petrol., 116: 433–447.

Iglesias Ponce de León, M. and Choukroune, P., 1980. Shear zones in the Iberian arc. J. Struct. Geol., 2: 63–68.

Julivert, M., Fontboté, J.M., Ribeiro, A. and Nabais Conde, L.E., 1972. Mapa Tectónico de la Península Ibérica y Baleares E. 1 : 1,000,000. Inst. Geol. Min. Esp. Madrid.

Kuijper, R.P., 1979. U–Pb systematics and the petrogenetic evolution of infracrustal rocks in the Paleozoic basement of Western Galicia, NW Spain. Verh. ZWO Lab. Isot. Geol. Amsterdam, 5: 1–101.

Kuijper, R.P., 1980. Precambrian U–Pb zircon ages from Western Galicia (NW Spain). Earth-Sci. Rev., 16: 313–316.

Lancelot, J.R., Allegret, A. and Iglesias-Ponce de León, M., 1985. Outline of Upper Precambrian and Lower Paleozoic evolution of the Iberian Peninsula according to U–Pb dating of zircons. Earth Planet. Sci. Lett., 74: 325–337.

Liñán, E. and Quesada, C., 1990. Ossa-Morena Zone. Stratigraphy. Rift Phase (Cambrian). In: R.D. Dallmeyer and E. Martínez García (Editors), Pre-Mesozoic Geology of Iberia. Springer-Verlag, Berlin, pp. 259–266.

Marcos, A. and Pulgar, J.A., 1982. An approach to the tectonostratigraphic evolution of the Cantabrian Foreland thrust and fold belt, Hercynian Cordillera of NW Spain. Neues Jahrb. Geol. Paläontol. Abh., 163: 256–260.

Marcos, A., Marquínez, J., Pérez-Estaún, A., Pulgar, J.A. and Bastida, F., 1984. Nuevas aportaciones al conocimiento de la evolución tectonometamórfica del Complejo de Cabo Ortegal (NW de Espana). Cuad. Lab. Xeol. Laxe, 7: 125–137.

Marquínez García, J.L., 1984. La geología del área esquistosa de Galicia Central (Cordillera Herciniana, NW de Espana). Mem. Inst. Geol. Min. Esp., 100, 231 pp.

Martínez, F.J. and Rolet, J., 1988. Late Paleozoic metamorphism in the northwestern Iberian peninsula, Brittany and related areas in southwestern Europe. In: A.L. Harris and D.J. Fettes (Editors), The Caledonian–Appalachian Orogen. Geol. Soc. London, Spec. Publ., 38: 611–620.

Martínez Catalán, J.R., 1983. Deformación heterogénea en los macizos graníticos de Sarria y Santa Eulalia de Pena (provincia de Lugo). Stud. Geol. Salmanticensia, 18: 39–63.

Martínez Catalán, J.R., 1990. A non-cylindrical model for the northwest Iberian allochthonous terranes and their equivalents in the Hercynian belt of Western Europe. Tectonophysics, 179: 253–272.

Martínez Catalán, J.R. and Arenas, R., 1992. Deformación extensional de las unidades alóctonas superiores de la parte oriental del Complejo de Ordenes (Galicia). Geogaceta, 11: 108–111.

Martínez Catalán, J.R., Pérez Estaún, A., Bastida, F., Pulgar, J.A. and Marcos, A., 1990. West Asturian–Leonese Zone. Structure. In: R.D. Dallmeyer and E. Martínez García (Editors), Pre-Mesozoic Geology of Iberia. Springer-Verlag, Berlin, pp. 103–114.

Martínez Catalán, J.R., Hacar Rodríguez, M.P., Villar Alonso, P., Pérez-Estaún, A. and González Lodeiro, F., 1992. Lower Paleozoic extensional tectonics in the limit between the West Asturian–Leonese and Central Iberian Zones of the Variscan Fold-Belt in NW Spain. Geol. Rundsch., 81: 545–560.

Martínez Catalán, J.R., Ayarza Arribas, P., Pulgar, J.A., Pérez-Estaún, A., Gallart, J., Marcos, A., Bastida, F., Alvarez-Marrón, J., González Lodeiro, F., Aller, J., Dañobeitia, J.J., Banda, E., Cordoba, D. and Comas, M.C., 1995. Results from the ESCI-N3.3 marine deep seismic profile along the Cantabrian continental margin. Rev. Soc. Geol. Esp., 8: 75–88.

Martínez Catalán, J.R., Arenas, R., Díaz García, F., Rubio Pascual, F.J., Abati, J. and Marquínez, J., 1996. Variscan exhumation of a subducted Paleozoic continental margin: The basal units of the Ordenes Complex, Galicia, NW Spain. Tectonics, 15: 106–121.

Massone, H.J. and Schreyer, W., 1987. Phengite geobarometry based on the limiting assemblage with K-feldspar, phlogopite and quartz. Contrib. Mineral. Petrol., 96: 212–224.

Matte, Ph., 1968. La structure de la virgation hercynienne de Galice (Espagne). Rev. Géol. Alp., 44: 1–128.

Munhá, J., Ribeiro, A. and Ribeiro, M.L., 1984. Blueschists in the Iberian Variscan Chain (Trás-os-Montes: NE Portugal). Comun. Ser. Geol. Portugal, 70: 31–53.

Ordóñez Casado, B., Gebauer, D., Schäfer, H.J., Gil Ibarguchi, J.I. and Peucat, J.J., 1996. A single subduction event at ca. 392 Ma for the ultramafic-mafic HP/HT-rocks of the Cabo Ortegal Complex. Geogaceta, 20: 489–490.

Parga Pondal, I., Matte, P. and Capdevila, R., 1964. Introduction à la géologie de l''Ollo de Sapo', Formation porphyroide antesilurienne du Nord Ouest de l'Espagne. Not. Com. Inst. Geol. Min. Esp., 76: 119–153.

Parga Pondal, I., Parga Peinador, J.R., Vegas, R. and Marcos, A., 1982. Mapa Geológico del Macizo Hespérico, Escala 1 : 500,000. Publ. Area de Xeoloxía e Minería, Sem. Estudos Galegos. Ed. do Castro. Coruña.

Paris, F. and Robardet, M., 1977. Paléogéographie et relations ibéro-armoricaines au Paléozoïque anté-carbonifére. Bull. Soc. Geol. Fr., 19: 1121–1126.

Perchuk, L.L., 1991. Derivation of a thermodynamically consistent set of geothermometers and geobarometers for metamorphic and magmatic rocks. In: L.L. Perchuk (Editor), Progress in Metamorphic and Magmatic Petrology. Cambridge University Press, Cambridge, pp. 93–112.

Pérez-Estaún, A., Bastida, F., Alonso, J.L., Marquínez, J., Aller, J., Alvarez-Marrón, J., Marcos, A. and Pulgar, J.A., 1988. A thin-skinned tectonics model for an arcuate fold and thrust belt: The Cantabrian Zone (Variscan Ibero-Armorican Arc). Tectonics, 7: 517–537.

Pérez-Estaún, A., Bastida, F., Martínez Catalán, J.R., Gutierrez Marco, J.C., Marcos, A. and Pulgar, J.A., 1990. West Asturian–Leonese Zone. Stratigraphy. In: R.D. Dallmeyer and E. Martínez García (Editors), Pre-Mesozoic Geology of Iberia. Springer-Verlag, Berlin, pp. 92–102.

Pérez-Estaún, A., Martínez Catalán, J.R. and Bastida, F., 1991. Crustal thickening and deformation sequence in the footwall to the suture of the Variscan Belt of NW Spain. Tectonophysics, 191: 243–253.

Peucat, J.J., Bernard-Griffiths, J., Gil Ibarguchi, J.I., Dallmeyer, R.D., Menot, R.P., Cornichet, J. and Iglesias Ponce de León, M., 1990. Geochemical and geochronological cross section of the deep Variscan crust: The Cabo Ortegal high-pressure nappe (northwestern Spain). Tectonophysics, 177: 263–292.

Pinto, M.S., 1984. O granito gnáissico de Fânzeres (Porto, Portugal). Idade e caracterizaçâo geoquímica geral. Mem. Not. Univ. Coimbra, 98: 231–242.

Platt, J.P., 1986. Dynamics of orogenic wedges and the uplift of high-pressure metamorphic rocks. Geol. Soc. Am. Bull., 97: 1037–1053.

Priem, H.N.A. and Den Tex, E., 1984. Tracing crustal evolution in the NW Iberian Peninsula through the Rb–Sr and U–Pb systematics of Paleozoic granitoids: a review. Phys. Earth Planet. Inter., 35: 121–130.

Priem, H.N.A., Boelrijk, N.A.I.M., Verschure, R.H. and Hebeda, E.H., 1965. Isotopic ages of two granites on the Iberian continental margin: the Traba granite (Spain) and the Berlenga granite (Portugal). Geol. Mijnbouw, 44: 353–353.

Priem, H.N.A., Boelrijk, N.A.I.M., Verschure, R.H., Hebeda, E.H. and Verdurmen, E.A.Th., 1970. Dating events of acid plutonism through the Paleozoic of the western Iberian Peninsula. Eclogae Geol. Helv., 63: 255–274.

Pulgar, J.A., 1980. Análisis e interpretación de las estructuras originadas durante las fases de replegamiento en la zona Asturoccidental-leonesa (Cordillera Herciniana, NW de España). Ph.D. Thesis, Univ. Oviedo, 334 pp.

Pulgar, J.A., 1981. La disolución por presión y el desarrollo del bandeado tectónico meso y microscópico en rocas metapelíticas de bajo grado del NW de España. Trab. Geol., 11: 147–190.

Quiroga, J.L., 1982. Estudio geológico del Paleozoico del W de Zamora. Trab. Geol., 12: 205–226.

Raase, P., 1974. Al and Ti contents of hornblende, indicators of pressure and temperature of regional metamorphism. Contrib. Mineral. Petrol., 45: 231–236.

Reuter, A., 1985. Korngröbenabhängigkeit von K–Ar Datierungen und Illit–Kristallinitat anchizonaler Metapelite und assozierter Metatuffe aus dem östlichen Reinischen Schiefergebirge. Göttinger Arb. Geol. Palaontol., 27: 91.

Ribeiro, A., 1974. Contribution à l'étude tectonique de Trás-os-Montes Oriental. Mem. Serv. Geol. Portugal, 24: 179 p.

Ribeiro, A., Pereira, E. and Dias, R., 1990. Central-Iberian Zone. Allochthonous Sequences. Structure in the northwest of the Iberian Peninsula. In: R.D. Dallmeyer and E. Martínez García (Editors), Pre-Mesozoic Geology of Iberia. Springer, Berlin, pp. 220–236.

Ribeiro, M.L., 1976. Considerações sobre uma ocorrência de crossite em Trás-os-Montes Oriental. Mem. Not. Univ. Coimbra, 82: 1–16.

Ries, A.C., 1979. Variscan metamorphism and K–Ar dates in the Variscan fold belt of S Brittany and NW Spain. J. Geol. Soc., London, 136: 89–103.

Rubio Pascual, F.J., Arenas, R. and Díaz García, F., 1993. Metapelitas de alta presión en la Unidad de Santiago (Complejo de Ordenes, NO del Macizo Ibérico). Geogaceta, 13: 101–104.

Sampson, S.D. and Alexander, E.C., 1987. Calibration of the interlaboratory $^{40}Ar/^{39}Ar$ dating standard, MMhb-1. Chem. Geol., 66: 27–34.

Santos Zalduegui, J.F., Schärer, U. and Gil Ibarguchi, J.I., 1995. Isotope constraints on the age and origin of magmatism and metamorphism in the Malpica–Tuy allochthon, Galicia, NW-Spain. Chem. Geol., 121: 91–103.

Santos Zalduegui, J.F., Schärer, U., Gil Ibarguchi, J.I. and Girardeau, J., 1996a. Origin and evolution of the Paleozoic Cabo Ortegal ultramafic–mafic complex (NW Spain): U–Pb, Rb–Sr and Pb–Pb isotope data. Chem. Geol., 129: 281–304.

Santos Zalduegui, J.F., Pin, C., Aranguren, A. and Gil Ibarguchi, J.I., 1996b. Application of specific extraction chromatographic methods to the Rb–Sr, Sm–Nd isotope study of geological samples: The Hombreiro–Santa Eulalia granite (Lugo, NW Spain). Geogaceta, 20: 495–497.

Schäfer, H.J., Gebauer, D., Gil Ibarguchi, J.I. and Peucat, J.J., 1993. Ion-microprobe U–Pb zircon dating on the HP/HT Cabo Ortegal Complex (Galicia, NW Spain): preliminary results. Terra Abstr., 5(4): 22.

Schermerhorn, L.J.G. and Kotsch, S., 1984. First occurrence of lawsonite in Portugal and tectonic implications. Comun. Ser. Geol. Portugal, 70: 23–29.

Serrano Pinto, M., Casquet, C., Ibarrola, E., Corretgé, L.G. and Portugal Ferreira, M., 1987. Síntese geocronológica dos granitoides do Maciço Hespérico. In: F. Bea, A. Carnicero, J.C. Gonzalo, M. López Plaza and M.D. Rodríguez Alonso (Editors), Geología de los granitoides y rocas asociadas del Macizo Hespérico. Rueda, Madrid, pp. 69–86.

Suárez, O., Ruiz, F., Galán, J. and Vargas, I., 1978. Edades Rb–Sr de granitoides del Occidente de Asturias (NW de España). Trab. Geol., 10: 437–442.

Teichmüller, M., Teichmüller, R. and Weber, K., 1979. Inkohlung und Illit–Kristallinitat — Vergleichende Untersuchungen im Mesozoikum und Paleozoikum von Westfalen. Fortschr. Geol. Rheinl. Westfalen, 27: 201–276.

Tollman, A., 1982. Großräumiger variszischer Deckenbau im Moldanubikum und neue Gedanken zum Variszikum Europas. Geotektonische Forsch., 64: 1–91.

Vacas, J.M. and Martínez Catalán, J.R., 1987. El sinforme de Alcañices en la transversal de Manzanal del Barco. Stud. Geol. Salmanticensia, 24: 151–175.

Valverde Vaquero, P. and Fernández, F.J., 1996. Edad de enfriamiento U/Pb en rutilos del Gneis de Chímparra (Cabo Ortegal, NO de España). Geogaceta, 20: 475–478.

Van Calsteren, P.W.C., Boelrijk, N.A.I.M., Hebeda, E.H., Priem, H.N.A., Den Tex, E., Verdurmen, E.A.T.H. and Verschure, R.H., 1979. Isotopic dating of older elements (including the Cabo Ortegal mafic–ultramafic complex) in the Hercynian Orogen of NW Spain: manifestations of a presumed Early Paleozoic Mantle plume. Chem. Geol., 24: 35–56.

Vogel, D.E., 1967. Petrology of an eclogite-and pyrigarnite-bearing polymetamorphic rock Complex at Cabo Ortegal, NW Spain. Leidse Geol. Med., 40: 121–213.

Weber, K., 1972. Notes on determination of illite crystallinity. Neues Jahrb. Mineral. Monatsh., 6: 267–276.

York, D., 1969. Least squares fitting of a straight line with correlated errors. Earth Planet. Sci. Lett., 5: 320–324.